Multiple Model-based Indoor Localization via Bluetooth Low Energy and Inertial Measurement Unit Sensors

Mohammadamin Atashi

A Thesis

in

The Department

of

Electrical and Computer Engineering

Presented in Partial Fulfillment of the Requirements

for the Degree of

Master of Applied Science (Electrical and Computer Engineering) at

Concordia University

Montréal, Québec, Canada

January 2021

CONCORDIA UNIVERSITY
SCHOOL OF GRADUATE STUDIES

This is to certify that the thesis prepared

By: Mohammadamin Atashi

Entitled: Multiple Model-based Indoor Localization via Bluetooth Low Energy and Inertial Measurement Unit Sensors

and submitted in partial fulfillment of the requirements for the degree of

Master of Applied Science (Electrical and Computer Engineering)

complies with the regulations of this University and meets the accepted standards with respect to originality and quality.

Signed by the final examining committee:

_____ Chair
      Dr. M.O. Ahmad

_____ External Examiner
      Dr. W. Lucia (CIISE)

_____ Internal Examiner
      Dr. M.O. Ahmad

_____ Supervisor
      Dr. A. Mohammadi (CIISE)

Approved by: _____
      Dr. Y.R. Shayan, Chair
      Department of Electrical and Computer Engineering

_____ 20___   _____
                     Dr. Mourad Debbabi, Interim Dean,
                     Gina Cody School of Engineering and
                     Computer Science

Abstract

Multiple Model-based Indoor Localization via Bluetooth Low Energy and Inertial
Measurement Unit Sensors

Mohammadamin Atashi

Ubiquitous presence of smart connected devices coupled with evolution of Artificial Intelligence (AI) within the field of Internet of Things (IoT) have resulted in emergence of innovative ambience awareness concepts such as smart homes and smart cities. In particular, IoT-based indoor localization has gained significant popularity, given the expected widespread implementation of 5G network, to satisfy the ever increasing requirements of Location-based Services (LBS) and Proximity Based Services (PBS). LBSs and PBSs have found several applications under different circumstances such as localization profiling for human resource management; navigation assistant applications in smart buildings/hospitals, and; proximity based advertisement and marketing. The focus of this thesis is, therefore, on design and implementation of efficient and accurate indoor localization processing and learning techniques. In particular, the thesis focuses on the following three positioning frameworks: (i) *Bluetooth Low Energy (BLE)-based Indoor Localization*, which uses the pathloss model to estimate the user's location; (ii) *Inertial Measurement Unit (IMU)-based Indoor Positioning*, where smart phone's 3 axis inertial sensors are utilized to iteratively estimate the headings and steps of the target, and; (iii) *Pattern Recognition-based Indoor Localization*, which uses Deep Neural Networks (DNNs) to estimate the performed actions and find the user's location. With regards to Item (i), the thesis evaluates effects of the orientation of target's phone, Line of Sight (LOS) / Non Line of Sight (NLOS) signal propagation, and presence of obstacles in the environment on the BLE-based distance estimates. Additionally, a fusion framework, combining Particle Filtering with K-Nearest Neighbors (K-NN) algorithm, is proposed and evaluated based on real

datasets collected through an implemented LBS platform. With regards to Item (ii), an orientation detection and multiple-modeling framework is proposed to refine Received Signal Strength Indicator (RSSI) fluctuations by compensating negative orientation effects. The proposed data-driven and orientation-free modeling framework provides improved localization results. With regards to Item (iii), the focus is on classifying actions performed by a user using Long Short Term Memory (LSTM) architectures. To address issues related to cumulative error of Pedestrian Dead Reckoning (PDR) solutions, three Online Dynamic Window (ODW) assisted LSTM positioning frameworks are proposed. The first model, uses a Natural Language Processing (NLP)-inspired Dynamic Window (DW) approach, which significantly reduces the computation time required for Real Time Localization Systems (RTLS). The second framework is developed based on a Signal Processing Dynamic Window (SP-DW) approach to further reduce the required processing time of the two stage LSTM based indoor localization. The third model, referred to as the SP-NLP, combines the first two models to further improve the overall achieved accuracy.

Acknowledgments

First and foremost, I would like to thank my exceptional supervisor, Dr. Arash Mohammadi, for his technical advice and excellent cooperation during my research. His support, immense knowledge, motivation, and spirit of adventure in regards research made this project possible. I thank you very much for all your guidance throughout my studies at Concordia University and I feel truly privileged to have worked with you. Besides my supervisor, I deeply express my gratitude to the committee members, Dr. Walter Lucia, Dr. M. Omair Ahmad, for evaluating the thesis and their thoughtful feedback.

My sincere thanks goes to my lovely family particularly my mother, who is a role model and a source of inspiration for me. This accomplishment would have not been possible without her endless support and faith in me throughout my years of study in life. I cannot express how grateful I am for all the sacrifices that she has done for me. To my father, Mohammad Mehdi, who believed me, supported me and encouraged me in myriad ways before he left this world. A warm and especial thanks to my sisters, Afrooz and Sepideh, for their emotional support, although we were mostly away from each other.

Last but by no means least, I thank my fellow lab mates for the stimulating discussions, and also for all the fun we have had in the last two years.

Contents

List of Figures

ix

List of Tables

Abbreviation

Abbreviation	Description
AI	Artificial Intelligence
ANN	Artificial Neural Networks
AU	Action Unit
BLE	Bluetooth Low Energy
CSV	Comma-Separated Values
DNN	Deep Neural Networks
DW	Dynamic Window
EF	Ellipsoid Fit
FC	Fusion Centre
GPS	Global Positioning System
iOS	iPhone Operating System
IMU	Inertial Measurement Unit
IoT	Internet of Things
IR	InfraRed
ISM	Industrial, Scientific, and Medical
KF	Kalman Filter
K-NN	K-Nearest Neighbor
LBS	Location based Services
LOS	Line of Sight
LPF	Low Pass Filter

LPS	Local Positioning Systems
LS	Long Step
LSTM	Long Short-Term Memory
MM	Multiple Model
MSE	Mean Square Error
NLOS	Non Line-of-Sight
NLP	Neural Language Processing
NN	Neural Network
NS	Normal Step
ODW	Online Dynamic Window
PBS	Proximity based Services
PCA	Principal Component Analysis
PDR	Pedestrian Dead-Reckoning
PF	Particle Filter
RFID	Radio-Frequency Identification
RNN	Recurrent Neural Networks
RSS	Received Signal Strength
RSSI	Received Signal Strength Indicator
RTLS	Real Time Localization System
SDK	Software Development Kit
SIS	Sequential Importance Sampling
SP	Signal Processing
SS	Short Step
STFT	Short Time Fourier Transform
SVM	Support Vector Machine
UHF	Ultra High Frequency
US	Ultrasonic
UWB	Ultra Wide Band

Chapter 1

Thesis Introduction

Recent developments and advancements in information processing, communication systems, networking, and cloud technologies have resulted in widespread use of reliable and affordable internet services around the world. As of 2013, there were 9 billion interconnected devices that are poised to reach more than 24 billion in 2021. This has resulted in evolution of an intriguing concept referred to as "The Internet of Things (IoT)" [1–5]. The basic motive behind the IoT concept is to provide advanced residential and enterprise solutions through the latest technologies in an energy efficient and reliable fashion without jeopardizing the service and comfort level for clients. The IoT paradigm rapidly gained ground in different applications of significant engineering importance including but not limited to medicare [6], smart home [7], vehicular networks [8], and smart public environments [9]. It is expected that IoT penetrates the everyday entities by 2025 including but not limited to furniture, home appliances, buildings, and hotels.

Within the IoT context, to establish trustworthiness into autonomous multi-agent networks, knowledge of the precise physical location of smart agents within indoor environments is critically needed [10–12]. However, localization is particularly challenging in Global Positioning System (GPS)-denied indoor environments. Localization in indoor environments is different not only in terms of the deployed sensors but also in terms of network design and signal propagation. Indoor positioning for providing Location-Based Services (LBSs) and Proximity Based Services (PBSs), where user's exact location is obtained satisfying high accuracy requirements, is of primary importance in IoT based services [13]. The user location, once obtained, can be leveraged to provide a

wide range of services such as context aware solutions, targeted advertisements, tenant assistance, and automated access, to name but a few. More particularly, LBSs play a vital role in emergence of many novel and intriguing IoT concepts such as smart homes and smart cities [23, 24]. Many indoor localization technologies, however, require proprietary infrastructure for network design. Recently, Local Positioning Systems (LPS) based on Bluetooth Low Energy (BLE), Inertial Measurement Unit (IMU), Ultra Wide Band (UWB), vision, sound, geomagnetic, and radio technologies have been investigated in great number of research works, attempting to implement a reliable indoor positioning system [25–28].

Of particular interest to this thesis is application of IoT-based technologies within the context of path trajectory estimation and proximity profiling in an indoor environment. In brief, the focus of the thesis is on the following three main localization frameworks when it comes to LBSs and PBSs in an indoor environment: (i) *BLE-based Indoor localization*, which uses the Received Signal Strength Indicator (RSSI) value to estimate the location of a BLE enabled device; (ii) *IMU-based Indoor Localization*, which iteratively estimates the position of an IMU-enabled agent (e.g., a smart phone) across its path trajectory, and; (iii) *Pattern Recognition-based Indoor Localization*, which attempts to recognize the actions performed by an agent using advanced and innovative sequential signal processing solutions.

Bluetooth Low Energy: Within the IoT context, BLE-based indoor localization [9, 13] for providing LBSs is of pivotal importance. In such methods, RSSI, as a measure of the distance of a device to a BLE sensor, is calculated dynamically using path loss model [3, 14, 15]. Despite the numerous advantages of BLE-based localization, such as low cost and low energy consumption of BLE sensors, RSSI values have drastic fluctuations adding random error and inaccuracy to such systems [16–18]. In fact, harsh and drastic fluctuations and noisy RSSI values would result in inaccurate distance estimation. To tackle this problem Kalman Filter (KF) is utilized to smooth the RSSI values and mitigate the effect of such errors on distance estimations [19]. Apart from the aforementioned challenges regarding RSSI values, there are other sources of noise negatively influencing BLE based systems such as orientation effect of receiver and transmitter of BLE packets, different RSSI ranges of mobile phones from different brands, and Line of Sight (LoS)/ Non Line of Sight (NLoS) signal propagation of BLE sensors on RSSI value to name but a few [20]. As

the initial step, this thesis evaluates the aforementioned influential parameters within the context of BLE-based indoor localization.

Inertial Measurement Unit: To address the aforementioned issues associated with BLE-based localization techniques, the thesis focus is on development of multiple-model IMU assisted positioning approaches. Generally speaking, IMU-based localization consists of two major components, i.e., heading estimation and step detection. Among different localization methods to analyze IMU data for the purpose of indoor positioning, Pedestrian Dead Reckoning (PDR) is the most popular and widely-used framework. In brief, based on the PDR algorithm, by determining heading and step length at each step, one can estimate the location of the user holding the smartphone over time. IMU-based positioning is prone to cumulative error, however, it can localize a target without dependence on any external hardware/sensors. Therefore, IMU-based frameworks are attractive solutions to be merged with BLE to enhance the overall localization accuracy. In this regard, the thesis proposes a Multiple Model (MM) framework to enhance the accuracy of RSSI based indoor positioning by compensating for the negative effects of orientation on the RSSI values.

Pattern Recognition-based Indoor Localization: For the third area (Item (iii) defined above), i.e., pattern recognition based indoor localization, the thesis proposes a framework that measures and validates the bodily acceleration and angular velocity patterns of the subject during indoor movements. The proposed architecture includes two Long Short Term Memory (LSTM) networks and a moving distance estimator. In fact, two separate LSTMs would be trained to learn the distinctive patterns of different movement and Action Units (AUs). The moving distance estimator predicts the final position of the subject based on the output of those two LSTMs. Conventional LSTM based indoor positioning solutions are not able to estimate the user's location in a real time or at least near real time fashion [21, 22]. In this thesis, however, the challenge of high computation requirement of two stage LSTM based indoor positioning is addressed by proposing two Online Dynamic Windows (ODWs). In fact, the initial goal of the thesis is to address the aforementioned challenges by proposing two different Natural Language Processing (NLP) and Signal Processing (SP) based online dynamic windows. In the first attempt, NLP inspired Dynamic Window (DW) is introduced which significantly reduces the computation time required for indoor positioning. In

5

another attempt to analyze the IMU sequential signal, Signal Processing Dynamic Window (SP-DW) is implemented which could further decrease the processing time for two stage LSTM based indoor localization. Finally, in order to establish a trade-off between running time latency and accuracy of the aforementioned DWs, a fusion ODW referred as SP-NLP based DW is proposed. The implementation of such framework renders near real time localization system.

1.1 Contributions

The main contributions [20, 43, 44] of the thesis research work are briefly outlined below:

(1) **Multiple Model BLE-based Tracking via Validation of RSSI Fluctuations under Different Conditions** [20]: A new BLE-based tracking framework is proposed, which evaluates the effects of different parameters on the RSSI fluctuations. In particular, effects of the following parameters on the RSSI values are investigated: (i) Users' orientation, different handling and gestures are tested; (ii) Users' distance to the BLE module; (iii) LOS or NLOS connection between the sensor and the Fusion Centre (FC), and; (iv) Presence of different obstacles between the BLE receiver and transmitter. Moreover, a part of the focus of the thesis is on investigating feasibility of micro-locating and tracking a person within a delimited physical space (e.g., an office building) via BLE signals. To perform BLE-based identification, localization, and tracking within indoor environments, a LBS platform is implemented consisting of the following two main sub-systems:

- *Acquisition sub-system*: The acquisition sub-system is responsible for collecting BLE packets and performing initial pre-processing and data aggregation tasks such as RSSI identification.

- *Fusion Centre*: The FC is in charge of executing the localization algorithm, storing results in the database, performing data analysis, and visualization. The collected data via the acquisition module is communicated to the FC, which consists of a processing module where tracking/localization algorithms are implemented; A local storage database, and; A local interface module to display and visualize processed data.

6

The implemented LBS platform is equipped with the following main properties: (i) Collecting synchronized measurements; (ii) Collecting measurements simultaneously from all the active locating devices installed in the physical space in a real-time fashion, and; (iii) Creating an efficient database for storing and accessing collected data with associated time-stamps and device IDs. Positional data are then collected in different areas using BLE enabled devices and are classified using learning methodologies to form fingerprints. The trained model is then coupled with a dynamic multi-model tracking algorithm. More specifically, the proposed BLE-based indoor localization framework consists of two integrated components: (i) A dynamic state estimation module based on Particle Filters (PF) [45,46], and; (ii) A K-nearest neighbour fingerprinting module that constructs (through the training phase) the RSSI map of the selected venue.

(2) **Multiple Model Framework to Evaluate and Eliminate Orientation Effects on RSSIs**: [43] The thesis has evaluated and modeled different possible effects associated with orientation of the transmitted signal on the estimated distance to enhance the accuracy of BLE-based indoor localization. In this regard, a MM framework is developed to eliminate the orientation effects. Furthermore, to minimize the effect of prior orientation of the smartphone on the distance estimation based on RSSI values, PDR technique is adopted to record the heading (orientation). In contrary to existing RSSI-based solutions that use a single path-loss model, the proposed framework consists of eight orientation-matched path loss models coupled with a multi-sensor and data-driven classification model that estimates the orientation of a handheld device with high accuracy of 99%. By estimating the orientation, we could mitigate the effect of orientation on the RSSI values and consequently improve RSSI-based distance estimates. In particular, the proposed data-driven and multiple-model framework is constructed based on over 10 million RSSI values and IMU sensor data collected via an implemented LBS platform.

(3) **Online Dynamic Window Assisted two stage LSTM for indoor positioning** [44]: An online two-stage LSTM indoor localization framework is proposed as a near Real Time Localization System (RTLS). The main objective is to obtain a trade-off between accuracy

7

and latency of the localization system to put one step forward towards having an efficient and respectively accurate indoor localization model. The proposed method consists of two phases, i.e.,

- *Offline Phase*: First, raw IMU values are collected using the embedded iPhone Operating System (iOS) Software Development Kit (SDK), and then smoothed via a KF or moving average filter. The labeled IMU sequential signal is then processed to be fed as the training input to the LSTM classifiers.

- *Online Phase*: In the online phase, the location of pedestrian would be estimated based on the performed actions. The inertial IMU data, however, is not splitted into AUs. To resolve this challenge, two innovative online dynamic windows are proposed to receive the sequential IMU data and split it into AUs. The proposed methods rely on advanced SP and NLP techniques. In conventional LSTM-based indoor localization methods, the AUs used to be splitted either by a fixed window or offline DW. The proposed SP and NLP inspired ODW mechanisms provide a fair trade off between the accuracy and processing time. An integrated SP-NLP based ODW is proposed to enhance the overall performance of the two-stage LSTM based indoor localization.

1.2   Thesis Organization

The rest of the thesis is organized as follows:

- Chapter 2 provides an overview of the literature on pre-processing units as well as BLE, IMU and pattern recognition based indoor localization techniques. In addition, this chapter provides the background required to follow developments presented in the reminder of the thesis.

- Chapter 3 considers the effects of different parameters on the RSSI values and distance estimation. In this regard, the chapter presents the multiple model BLE-based tracking framework, which validates the RSSI fluctuations in distance estimation.

- Chapter 4 elaborates more on the orientation effects on distance estimation. In this regard, a multiple-model estimation framework is proposed to analyze and address effects of orientation of a BLE-enabled device on indoor localization accuracy. The proposed data-driven RSSI-IMU fusion framework is constructed based on over 10 million RSSI values and IMU sensor data collected via an implemented LBS platform.

- Chapter 5 considers the application of pattern recognition in indoor localization and presents two-stage LSTM-based indoor positioning techniques. Three online dynamic windows (e.i., SP DW, NLP DW, NLP-SP DW) assisted are proposed for near-online indoor positioning.

- Chapter 6 concludes the thesis and provides potentials directions for future research works.

Chapter 2

Literature Review and Background

As mentioned previously in Chapter 1, one of the prominent factors in service differentiation and personalized control systems is the ambient intelligence. Thus, having the knowledge of current location of a subject can facilitate and ease the chores in various domains (e.g., military, medicine, public safety services to name but a few). Owing to the conspicuous and fast-paced advancements in outdoor localization systems, many objects (things) in outdoor spaces can be inter-connected and have knowledge about precise location of one another in a designed network. As a promising advancement in this domain, GPS provides real-time geographical location information based on the use of satellites. Embedded in all smart phones, GPS can fully meet the needs of outdoor localization.

Recent developments and advancements in IoT domain, low power wireless networks, and processing methodologies have resulted in the emergence of several different and innovative indoor localization technologies, including InfraRed (IR) systems [47], Ultrasonic (US) systems [48], Radio-Frequency IDentification (RFID) [48], ZigBee [49], WiFi [55], BLE [56], UWB [57] and Optical-based frameworks [49]. The aim in this domain is to identify, track, and monitor intelligent agents in an autonomous multi-agent systems. These systems share several common underlying properties, such as being sensitive to multipath effects, high costs and complexity and in some cases not being readily available [55]. Considering indoor localization, however, a fully scalable, accurate and affordable indoor positioning approach is yet to be proposed. In this chapter, a detailed review on the most widely used conventional indoor positioning frameworks is presented. It is worthy to

mention that this chapter provides the background required to follow developments presented in the reminder of the thesis.

2.1 BLE-based Indoor Localization

To localize a person inside an indoor venue, typically, digital chips referred to as "BLE Beacons" are utilized. In recent years, such BLE-enabled devices have gained increased popularity [9, 13] mainly due to the ongoing interest in the IoT concept [2, 5, 8] and the progression made in the Bluetooth technology. The practicality of Bluetooth signals in the indoor environments for positioning purposes [1, 4, 41], particularly after the introduction of the new specifications of the BLE (BLE v5.0 and v5.1), increased significantly. In order to perform micro-location based on BLE tags, the main-stream methodology is to analyze the RSSI values [14, 16, 38]. Basically, RSSI is regarded as an important parameter, representing the distance of a user to BLE chip in an indoor environment [3, 14, 15, 58]. As one of the most widely used indoor localization methods, RSSI of BLE signals can be related to the distance between the transmitter and receiver of the digital packet using the path loss model. Stand alone RSSI based localization models, however, fail to provide acceptable indoor localization accuracy. The low accuracy of the algorithms implemented based on the RSSI signals, mainly stems from their high fluctuations [16]. Apart from drastic and inevitable RSSI fluctuations, there are other important parameters affecting accuracy of RSSI-based indoor localization.

2.1.1 Bayesian Filtering

Throughout the thesis, the following notations are used: non-bold capital letter X denotes a scalar variable, lowercase bold letter $\boldsymbol{x}$ represents a vector, and capital bold letter $\boldsymbol{X}$ denotes a matrix.

We consider an indoor localization scenario where the first goal is to test and validate effects of different parameters on the RSSI values. The second goal is to perform information fusion and estimate trajectory of a single user walking within the surveillance venue equipped with $N_b > 1$

number of BLE beacons (sensors). The following general non-linear state-space model is considered

$$\boldsymbol{x}_k \quad = \boldsymbol{f}\big(\boldsymbol{x}_{k-1}\big) + \boldsymbol{w}_k \tag{2.1}$$

$$\text{and} \quad \boldsymbol{z}_k \quad = \begin{bmatrix} h^{(1)}(\boldsymbol{x}_k) + v_k^{(1)} \\ \vdots \\ h^{(N_b)}(\boldsymbol{x}_k) + v_k^{(N_b)} \end{bmatrix}, \tag{2.2}$$

where $\boldsymbol{z}_k \in \mathbb{R}^{N_b}$ denotes the sensor's measurement vector at iteration k; $\boldsymbol{x}_k \in \mathbb{R}^{N_x}$ is the state vector; functions $\boldsymbol{f}$ and $\boldsymbol{h}$, respectively, are the state and observation models; terms $\boldsymbol{w}_k$ and $\boldsymbol{v}_k$ represent the forcing terms and uncertainties in the observation model, and assumed to be mutually uncorrelated white Gaussian noises with known covariance matrices $\boldsymbol{Q}_k > 0$ and $\boldsymbol{R}_k > 0$, respectively.

Generally speaking, to track a target within indoor enurements via BLE measurements, a Bayesian filter is developed based on Eqs. (2.1)-(2.2), which has the following two key steps:

(i) *Prediction Step*: In this step, the a-priory density at time k is calculated, i.e.,

$$P(\boldsymbol{x}_k|\boldsymbol{z}_{1:k-1}) = \int P(\boldsymbol{x}_k|\boldsymbol{x}_{i:k-1})P(\boldsymbol{x}_{k-1}|\boldsymbol{z}_{1:k-1})d\boldsymbol{x}_{k-1}. \tag{2.3}$$

(ii) *Update Step*: In this step, after receiving measurements at time k, the a-priory density is updated using Bayesian rule as follows

$$P(\boldsymbol{x}_k|\boldsymbol{z}_{1:k}) = \frac{P(\boldsymbol{z}_k|\boldsymbol{x}_k)P(\boldsymbol{x}_k|\boldsymbol{z}_{1:k-1})}{P(\boldsymbol{z}_k|\boldsymbol{z}_{k-1})}, \tag{2.4}$$

where $P(\boldsymbol{z}_k|\boldsymbol{z}_{k-1})$ depends on $P(\boldsymbol{z}_k|\boldsymbol{x}_k)$, and

$$P(\boldsymbol{x}_k|\boldsymbol{z}_{k-1}) = \int P(\boldsymbol{z}_k|\boldsymbol{x}_k)P(\boldsymbol{x}_k|\boldsymbol{z}_{k-1})d\boldsymbol{x}_{k-1}. \tag{2.5}$$

Kalman Filter: In KF formulation, it is assumed that the posterior probability distribution at time k is Gaussian. Furthermore, KF is based on linear state-space version of Eqs. (2.1) and (2.2), which

can be written as follows

$$\boldsymbol{x}_k \;=\; \boldsymbol{F}\boldsymbol{x}_{k-1} + \boldsymbol{w}_k \tag{2.6}$$

$$\boldsymbol{z}_k \;=\; \boldsymbol{H}\boldsymbol{x}_{k-1} + \boldsymbol{v}_k, \tag{2.7}$$

where $\boldsymbol{w}_k = \mathbb{N}(0, \boldsymbol{Q})$ and $\boldsymbol{v}_k = \mathbb{N}(0, \boldsymbol{R})$. The prediction stage of the KF is then implemented as follows

$$\hat{\boldsymbol{x}}_k^- \;=\; \boldsymbol{F}\hat{\boldsymbol{x}}_{k-1} \tag{2.8}$$

$$\boldsymbol{P}_k^- \;=\; \boldsymbol{F}\boldsymbol{P}_{k-1}\boldsymbol{F}^T + \boldsymbol{Q}, \tag{2.9}$$

where $\hat{\boldsymbol{x}}_{k-1}$, is the posterior state estimate at time $(k-1)$ given observations up to and including time $(k-1)$. Matrix $\boldsymbol{P}_{k-1}$ is posterior error covariance matrix (a measure of the estimated accuracy of the state estimate) at time $(k-1)$. The update step of the KF is then implemented as follows

$$\boldsymbol{K}_k \;=\; \boldsymbol{P}_k^- \boldsymbol{H}^T (\boldsymbol{H}\boldsymbol{P}_k^-\boldsymbol{H}^T + \boldsymbol{R})^{-1} \tag{2.10}$$

$$\hat{\boldsymbol{x}}_k \;=\; \hat{\boldsymbol{x}}_k^- + \boldsymbol{K}_k(\boldsymbol{z}_k - \boldsymbol{H}\hat{\boldsymbol{x}}_k^-) \tag{2.11}$$

$$\text{and} \quad \boldsymbol{P}_k \;=\; (\boldsymbol{I} - \boldsymbol{K}_k\boldsymbol{H})\boldsymbol{P}_k^-. \tag{2.12}$$

Particle Filter: The particle filtering algorithm is based on the principle of Sequential Importance Sampling (SIS), which is a sub-optimal approach for implementing recursive Bayesian estimation (Eqs. (2.3)-(2.5)) through Monte Carlo simulations. Importance sampling is an approach to evaluate an integral, e.g.,

$$\mathbb{E}\{h(x)\} = \int h(x)p(x|z)dx = \int h(x)\frac{q(x|z)}{q(x|z)}q(x|z)dz \tag{2.13}$$

where $\mathbb{E}\{\cdot\}$ denotes expectation. A numeric way to compute $\mathbb{E}\{h(\boldsymbol{x}_k)\}$ is to draw N_p random samples (vector particles) $\{\mathbb{X}_k^i\}_{i=1}^{N_p}$ from a proposal distribution $q(\boldsymbol{x}_k|\boldsymbol{z}_k)$ with normalized weights W_k^i, for $(1 \le i \le N_p)$, associated to the vector particles. Assuming that the evolution of the state

13

variables is Markovian, the weights are updated as follows

$$W_k = W_{k-1} \frac{p(\boldsymbol{z}_k|\boldsymbol{x}_k)p(\boldsymbol{x}_k|\boldsymbol{x}_{k-1})}{q(\boldsymbol{x}_k|\boldsymbol{x}_{0:k-1}, \boldsymbol{z}_{1:k})}, \tag{2.14}$$

where $\boldsymbol{z}_{1:k}$ includes all observations from iteration 1 to k. A similar notation is used for the remaining variables. A common choice for the proposal distribution is the transition density, $p(\boldsymbol{x}_k|\boldsymbol{x}_{k-1})$, where the weights are pointwise evaluation of the likelihood function at the particle values. In brief, the PF approximates the posterior distribution $P(\boldsymbol{x}_k|\boldsymbol{z}_k)$ using a set of N_p particles $\{\mathbb{X}_k^i\}_{i=1}^{N_p}$ and their associated normalized weights W_k^i. More details on PF is available in Reference [45].

2.1.2 Pathloss Model

As one of the most widely used indoor localization methods, RSSI value of BLE signal can be related to the distance between the transmitter and receiver of digital packets using the path loss model [14, 62]. More specifically, the RSSI values obtained from the jth active BLE beacon, for $(1 \leq j \leq N_b)$, make the observation equation based on the pathloss model as follows

$$Z_k^{(j)} = \underbrace{-10\,N\,\log(\frac{D_k^{(j)}}{D_0}) + C_0}_{h^{(j)}(\boldsymbol{x}_k)} + v_k^{(j)}, \tag{2.15}$$

where

$$D_k^{(j)} = \sqrt{(X_k - X_k^{(j)})^2 + (Y_k - Y_k^{(j)})^2}, \tag{2.16}$$

with $\boldsymbol{x}_k^{(j)} = [X_k^{(j)}, Y_k^{(j)}]^T$ denoting 2-D location of the jth sensor; D_0 is the reference distance; C_0 is the average RSSI value at reference distance; N is the pathloss exponent. As mentioned in Chapter 1, pathloss-based solutions are prone to multipath fading and drastic fluctuations in the indoor environment. To deal with multipath signal propagation, one needs to resort to multitude of advanced signal processing solutions to either deal with multipath propagation or even exploit the presence of multipath effect, e.g., using KF and PFs [16]. The drastic and random fluctuations of RSSI values make the system vulnerable to high level of noise and error [20, 59]. To mitigate

14

the effect of drastic fluctuations in RSSI values, different localization methods such as fingerprint-ing [60], tri-lateration [62] and triangulation [61] techniques have been deployed. Alternatively, some solutions are developed based on machine learning schemes such as NNs [39,40]. Although very recently BLE-based indoor localization via NNs has been explored, such solutions for RSSI-based localization are still in their infancy.

Fingerprinting: Apart from Bayesian filtering and the pathloss approach, to mitigate effects of drastic fluctuations in RSSI value, fingerprinting technique has also been deployed. Fingerprinting is a widely used approach [50–54], which at the first phase (offline phase) gathers training data (in localization purposes RSSI, magnetic or Wi-Fi data) within pre-determined zones. Once the suit-able amount of data for each zone is collected, the algorithm in the second phase (online phase) estimates a particular location pattern by matching the new data with the training data stored in the database. The whole process of collecting data for each pre-determined zone and implement-ing RTLS based on the reported data is considered as a time consuming and non-efficient indoor localization technique.

2.2 IMU-based Indoor Localization

Due to ubiquitous integration of IMU in smartphones, there has been an ongoing surge of inter-est on utilization of inertial data to estimate the location of smart phones in indoor environments. Relying on local deployed sensors and local central processing unit, the deployment of such sys-tems is considered as a very efficient way to localize a user without utilizing external, proprietary, expensive hardware or wearable sensors [43, 63]. The IMU module in smartphones consists of 3-axis accelerometer, 3-axis magnetometer and 3-axis Gyroscope. Due to the high level of noise and sudden drifts in IMU signals, the raw data reported by IMU sensors should be pre-possessed before utilization to localize a target. The details of the required pre-processing steps are provided below:

(1) **Moving Average (Smoothing) Filter:** Typically, the raw data reported by IMU sensors are prone to noise and sudden drifts, adding inaccuracy to the localization techniques. In order to mitigate, and if applicable remove the level of drastic fluctuations in raw inertial reports of 3-axis accelerometer, magnetometer and gyroscope, the data is smoothed using a low pass
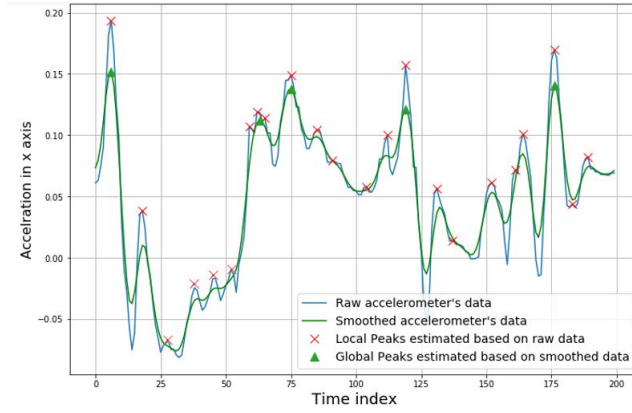
Figure 2.1: Raw and smoothed inertial reports and illustration of a peak detection algorithm.

filter or a moving average filter. The moving average filter used in this thesis is given by

$$x_f(n)_\alpha = \frac{1}{N} \sum_{k=0}^{N-1} \boldsymbol{x}_\alpha(n+k); \alpha = \{a_{x,y,z}, g_{x,y,z}\}, \tag{2.17}$$

where α represents the bodily acceleration $a_{x,y,z}$ and angular movements $g_{x,y,z}$ of the subjects in the X, Y, and Z axes, respectively. Term N is the number of indexes in a sample inertial signal. Fig. 2.1 illustrates the raw and smoothed versions of a sample accelerometer's data. The smoothed inertial data can be used as the input to signal processing (i.e., step and zero cross point detection) and pattern recognition (i.e., Recurrent Neural Network (RNN), LSTM-based AU classification) techniques.

(2) **Magnetometer Calibration Unit**: As stated above, smartphone's IMU unit consists of 3-axis accelerometer, 3-axis gyroscope, and 3-axis magnetometer. All IMU sensors report data with respect to the 3 orthogonal and pre-defined axis in the smart phone. Due to soft-iron and hard-iron effects, magnetometer is vulnerable to noise and error. In such cases, a calibration unit should be adopted on the magnetometer's data such as Ellipsoid Fit (EF) method [35]. This calibration unit estimates all parameters of the error model and then compensate the errors caused by soft and hard iron interferences. The absolute heading angle estimated by magnetometer reports is unreliable since the magnetic field received by a smartphone has high correlation to the venue, surrounding walls, and the presence of other magnetic fields in the venue. Hard iron and soft iron effects stem from the magnetometer's distorted readings.
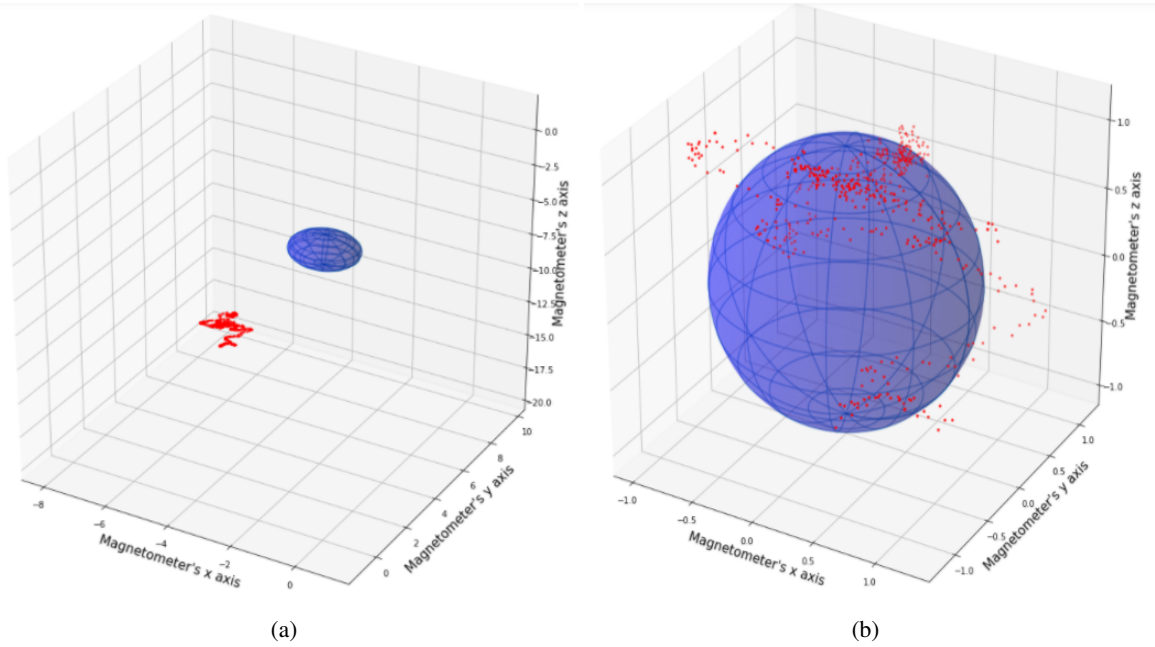
Figure 2.2: EF calibration unit for magnetometer. (a) Raw and error-prone magnetometer data. (b) EF calibrated and error compensated magnetometer data.

Although there has been attempts to compensate the error caused by external magnetic fields via implementing calibration units such as ellipsoid fit magnetometer calibration unit, the attempts are not fully successful to significantly decrease the effects of such hurdles. Fig. 2.2(a) shows the raw, distorted, and noisy magnetometer's readings. In Fig. 2.2(b), by applying the EF calibration technique on magnetometer's data, the error from this inertial sensor reports has been compensated. All of the mentioned challenges illustrate unreliable and error-prone measurement picture of magnetometer-based heading estimation. Thus, in state-of-the-art localization methods, the focal point in heading estimation is to utilize the information in gyroscope reports to determine the direction of the target.

2.2.1   Pedestrian Dead Reckoning

Among IMU based indoor localization techniques, PDR is the most widely used technique to iteratively estimate the current location of an IMU enabled object in indoor environments. Starting from a known position, successive displacement of the object is estimated using the two major heading estimation and step detection techniques, leading to the current Cartesian coordinates (i.e.,

X and Y coordinates) of the user, as follows

$$
\begin{bmatrix}
X_k \\
\Delta X_k \\
Y_k \\
\Delta Y_k
\end{bmatrix}
=
\underbrace{\begin{bmatrix}
1 & \Delta t & 0 & 0 \\
0 & 1 & 0 & 0 \\
0 & 0 & 1 & \Delta t \\
0 & 0 & 0 & 1
\end{bmatrix}}_{\boldsymbol{F}_k}
\begin{bmatrix}
X_{k-1} \\
\Delta X_{k-1} \\
Y_{k-1} \\
\Delta Y_{k-1}
\end{bmatrix}
+ \boldsymbol{w}_k.
\tag{2.18}
$$

The coordinates of posterior steps are highly dependent on the location of the prior steps, adding an inevitable and increasing cumulative error to the PDR-based positioning systems. In fact, an inaccurate heading estimation or false step detection will directly influence the faulty location estimation in the posterior steps. Furthermore, the Cartesian coordinates and the heading of the user at the starting point are regarded as strict requirements of the PDR method. Basically, PDR-based indoor localization approach consists of the following two major "Heading estimation" and "Step detection" steps:

(i) *Step Detection*: The distance travelled by the user holding an IMU enabled device can be represented by her/his number of steps. Therefore, an accurate step detection algorithm can render better positioning estimation. Although number of steps taken by a user in an indoor environment can be estimated by counting the positive going, zero crossings of a low-pass filtered version of the signal [33, 64, 65], the strongest indication of the step specific peak signature is represented on the vertical axis relative to ground [37, 66]. However, the vertical signal component may be distributed among all three accelerometer axis depending on the present orientation and attitude of the smartphone. To resolve the aforementioned challenge, the axis with highest variation can be selected for step detection evaluation process. Adopting adjacent peak selection, our implemented step detection process is given by

$$
\Upsilon^i \;=\; \begin{cases}
\Upsilon^i \geq \tau \longrightarrow \text{Step} \\
\Upsilon^i \leq \tau \longrightarrow \text{Local Peak,}
\end{cases}
\tag{2.19}
$$

where the magnitude of consecutive local acceleration peaks (Υ^i) are subject to a defined

threshold (τ), which is an empirically determined constant value. Additionally, to insure a valid global peak (step), the time interval between two consecutive steps should fall between 120ms to 400ms. Fig. 2.1 depicts the estimated steps based on smoothed version of acceleration signal.

(ii) *Heading Estimation Unit*: In order to determine the heading of a planar smartphone, first pitch and roll angles are directly calculated based on the accelerometer's readings as follows

$$P = \arctan \frac{A_y}{\sqrt{A_x{}^2 + A_z{}^2}} \tag{2.20}$$

$$\text{and} \quad R = \arctan \frac{-A_x}{A_z}. \tag{2.21}$$

Once the pitch and roll angles for each step are calculated, yaw angle can be determined as follows

$$X_h = M_x \cos{(P)} + M_y \sin{(P)} \sin{(R)} + M_z \sin{(P)} \cos{(R)}$$

$$\text{and} \quad Y_h = M_y \cos{(R)} + M_z \sin{(R)}, \tag{2.22}$$

where

$$P = \arctan\{A_y/\sqrt{A_x{}^2 + A_z{}^2}\} \tag{2.23}$$

$$R = \arctan\{(-A_x)/A_z\} \tag{2.24}$$

$$\text{and} \quad Yaw^{\text{Rad}} = \arctan -(\frac{Y_h}{X_h}). \tag{2.25}$$

In the case that the user holds the device in a plenary position, yaw angle is regarded as the heading angle of the device. Fig. 2.3 depicts a brief overview of the aforementioned IMU heading estimation approach. Yaw-based representation of heading estimation, in fact, is not practical when the smart phone is swinging in the user's hand or in rests in her/his pocket. To consider the effect of the smartphone's position on the heading estimation algorithm, Principal Component Analysis (PCA) and PCA-based method coupled with global accelerations
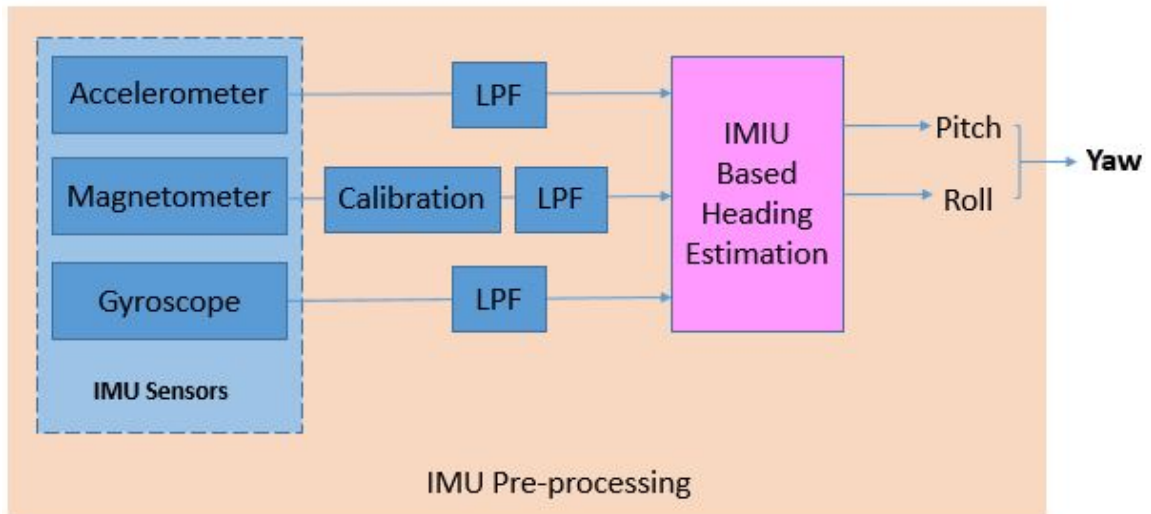
19

Figure 2.3: Heading estimation by IMU.

(PCA-GA) are employed in conventional PDR-based localization researches. These meth-
ods are, however, still error-prone since magnetometer is vulnerable and easily influenced by
interferences caused by external magnetic fields.

In addition to 3-axis accelerometer, 3-axis magnetometer, and 3-axis Gyroscope, barometer and
light sensors can be used to report the altitude of the smartphone and perform better proximity
localization.

2.3   Pattern Recognition-based Indoor Localization

Due to the drastic and high level of fluctuations in sequential signal reported by inertial sensors
the aforementioned techniques, however, are highly prone to error, leading to false and inaccurate
step detection. The error in step detection (false either positive or negative labels) leads to distorted
and error-prone path estimation. To address the aforementioned issues, recently Machine Learning
(ML) and Deep Neural Network (DNN) based solutions [21, 22, 70, 71] are proposed commonly
based on the Long Short-Term Memory architecture. DNN-based techniques can also perform AU
classification (such as long step, short step, left turn, right turn, stop) and movement statuses (such as
walking, running, or stop). Real-time implementation of such an approach, however, is impossible

due to the excessive tensor based computational power required for the model's dynamic windowing approach. In the recent ML based methods however, there are an ongoing attempts to reduce the probability of false steps using ML based feature extraction techniques. In addition, in more recent research works, the extracted numerical features such as acceleration magnitude, maximum value, minimum value and variance are then used in neural networks as input training patterns.

2.3.1 Machine Learning-based Pattern Recognition

Pedestrian dead Reckoning approaches based on the motion mode recognition of the smart phone were deployed to estimate the user's location. The approaches to deploy a flexible and scalable PDR positioning have flourished to the point that modeling the arbitrary combination of phone pose and movement state (walking, running, upstairs, downstairs) was proposed. Physical differences of different individuals such as height and step length added an adaptive point to the proposed algorithms to establish the step length adaptive PDR localization techniques. Low pass filtered and smoothed sequential data reported by IMU sensors are insufficient to distinguish various motion modes. Thus, there is a need for feature extraction from filtered IMU data using a sliding window. The length of the sliding window is typically fixed, which can include several steps. Once the sliding window is applied on the sequential data, it provides an estimated label (motion mode) for each scanned segment of the data. In fact, the periodic features of steps can be modeled in prior steps to predict the occurrence of posterior steps with a higher confidence rate. As proven in previous research works, time domain features such as acceleration and velocity's variance and mean values, and frequency domain features such as Short Time Fourier Transform (STFT) are not reliable enough to detect the posterior steps in the path trajectory. The extracted features are handcrafted, and thus they do not sufficiently represent the input data. Therefore, it is a difficult task to obtain the best representative handcrafted features from the input data for classification. The most recent articles, therefore, have gone beyond the conventional feature extraction solutions to extract deep features from the sequential inertial signal.

2.3.2 Two Stage LSTM-based Indoor Localization

As mentioned in Section 2.2, analyzing the gait information in IMU data, step and heading based indoor localization techniques have strict limitations and deficiencies making them non reliable positioning systems. To address the aforementioned challenges from a practical Artificial Intelligence(AI) perspective, deep models have been emerged. Typically, deep learning methods render a structure in which end-to-end learning, automated feature extraction and classification, is performed instead of using handcrafted features. Due to the ongoing developments in sequential data processing using ML models and ANNs, the solution to many challenges associated with traditional IMU based indoor positioning techniques are being solved by modeling indoor localization experiments on AU recognition and classification models. Hence, to end up with reasonably accurate positioning system the raw data reported by IMU sensors should be processed to be used as the input to pattern recognition models.

The LSTMs are considered as the state-of-the-art technique for sequence learning. The LSTM was first introduced by Hochreiter and Schmidhuber, and were further refined and popularized in the following year. The LSTMs are designed to overcome the vanishing and exploding gradient problem of the traditional Recurrent Neural Networks (RNNs). This is achieved by introducing a memory state and multiple gating functions, that provide a memory-based architecture to control the write, read, and removal (forget) of the information written on the memory state. Consequently, the LSTMs have been successfully applied in wide range of applications, including speech recognition, natural language processing, handwriting recognition, and image captioning to name a few.

Generally speaking, the LSTM model takes a single time window as the input and learns how to model that sequence with respect to the provided label. The sequence lengths are considered to be of fixed length and the structure of the incorporated LSTM is many to one. The output and the cell states have the same vector size, which is defined by the number of nodes in the cell. When the number of nodes is equal to m, the output of the LSTM cell is $h^t \in \mathbb{R}^{m \times 1}$ and the cell state is $c^t \in \mathbb{R}^{m \times 1}$. The output h^{t-1} and the hidden state c^{t-1} of the LSTM cell at time $(t) - 1$ will be the input to the LSTM at time (t) in addition to the sensor data x^t. The information flow of the internal cell unit is controlled by a gating logic consisting of three gates: (i) The input gate $i^t \in \mathbb{R}^{m \times 1}$,

which determines what information based on ($\boldsymbol{h}^{t-1}$ and $\boldsymbol{x}^t$) will be forward to the memory cell; (ii) The output gate $\emptyset^t \in \mathbb{R}^{\boldsymbol{m} \times 1}$, which controls what information will be passed to the next time step, and; (iii) The forget gate $\boldsymbol{f}^t \in \mathbb{R}^{\boldsymbol{m} \times 1}$, which controls how the memory cell will be updated. The following equations describe the implementation and update of the memory cells in the LSTM layer at every time step (t)

$$\boldsymbol{i}^t = \sigma(\boldsymbol{W}^{(i)}\boldsymbol{x}^t + U^{(i)}\boldsymbol{h}^{t-1} + \boldsymbol{b}^{(i)}), \tag{2.26}$$

$$\emptyset^t = \sigma(\boldsymbol{W}_o\boldsymbol{x}^t + U_o\boldsymbol{h}^{t-1} + \boldsymbol{b}_o), \tag{2.27}$$

$$\boldsymbol{f}^t = \sigma(\boldsymbol{W}_f\boldsymbol{x}^t + U_f\boldsymbol{h}^{t-1} + \boldsymbol{b}_f), \tag{2.28}$$

$$\boldsymbol{a}^t = \tan(\boldsymbol{W}_c\boldsymbol{x}^t + U_c\boldsymbol{h}^{t-1} + \boldsymbol{b}_c), \tag{2.29}$$

$$\boldsymbol{c}^t = \boldsymbol{f}^t \circ \boldsymbol{c}^{t-1} + \boldsymbol{i}^t \circ \boldsymbol{a}^t, \tag{2.30}$$

$$\boldsymbol{h}^t = \emptyset^t \circ \tan(\boldsymbol{c}^t), \tag{2.31}$$

where $\boldsymbol{W}^{(i)}, \boldsymbol{W}_o, \boldsymbol{W}_f, \boldsymbol{W}_c \in \mathbb{R}^{\boldsymbol{m} \times (l)}$, and $U^{(i)}, U_o, U_f, U_c \in \mathbb{R}^{\boldsymbol{m} \times \boldsymbol{m}}$ are weight matrices; Terms $\boldsymbol{b}^{(i)}, \boldsymbol{b}_o, \boldsymbol{b}_f, \boldsymbol{b}_c \in \mathbb{R}^{\boldsymbol{m} \times 1}$ are bias vectors; $\sigma(\cdot)$ denotes the sigmoid activation function; Operator "$\circ$" denotes the Hadamard product (element-wise multiplication of two vectors), and; $\tan(\cdot)$ represents element-wise hyperbolic tangent activation function.

Chapter 3

Multiple Model BLE-based Tracking via Validation of RSSI Fluctuations under Different Conditions

Of particular interest to this chapter, is indoor positioning via integration of information fusion, localization, and tracking technologies with IoT devices equipped with sensing, processing, and BLE communication capabilities. In particular, the objective is development of advanced signal processing and machine learning solutions to micro-locate and track a person within a delimited physical space (e.g. building) using BLE locating infrastructure installed within this space. As stated previously in Chapter 1, different environmental parameters can negatively influence the RSSI fluctuations. In this regard and as the first step, the chapter focuses on evaluation and validation of RSSI fluctuations under different environmental conditions. Therefore, the first goal of the chapter is to implement a LBS platform consisting of two main sub-systems, i.e., acquisition sub-system, and the FC. The second goal of the chapter is to test and validate effects of different parameters on the RSSI values and on the tracking performance. Based on real experiments, the implemented LBS platform shows potential capabilities for incorporation of different fusion frameworks and providing accurate tracking results. The reminder of the chapter is organized as follows: Section 3.1 formulates the problem and develops the BLE-based estimation framework. Experimental results
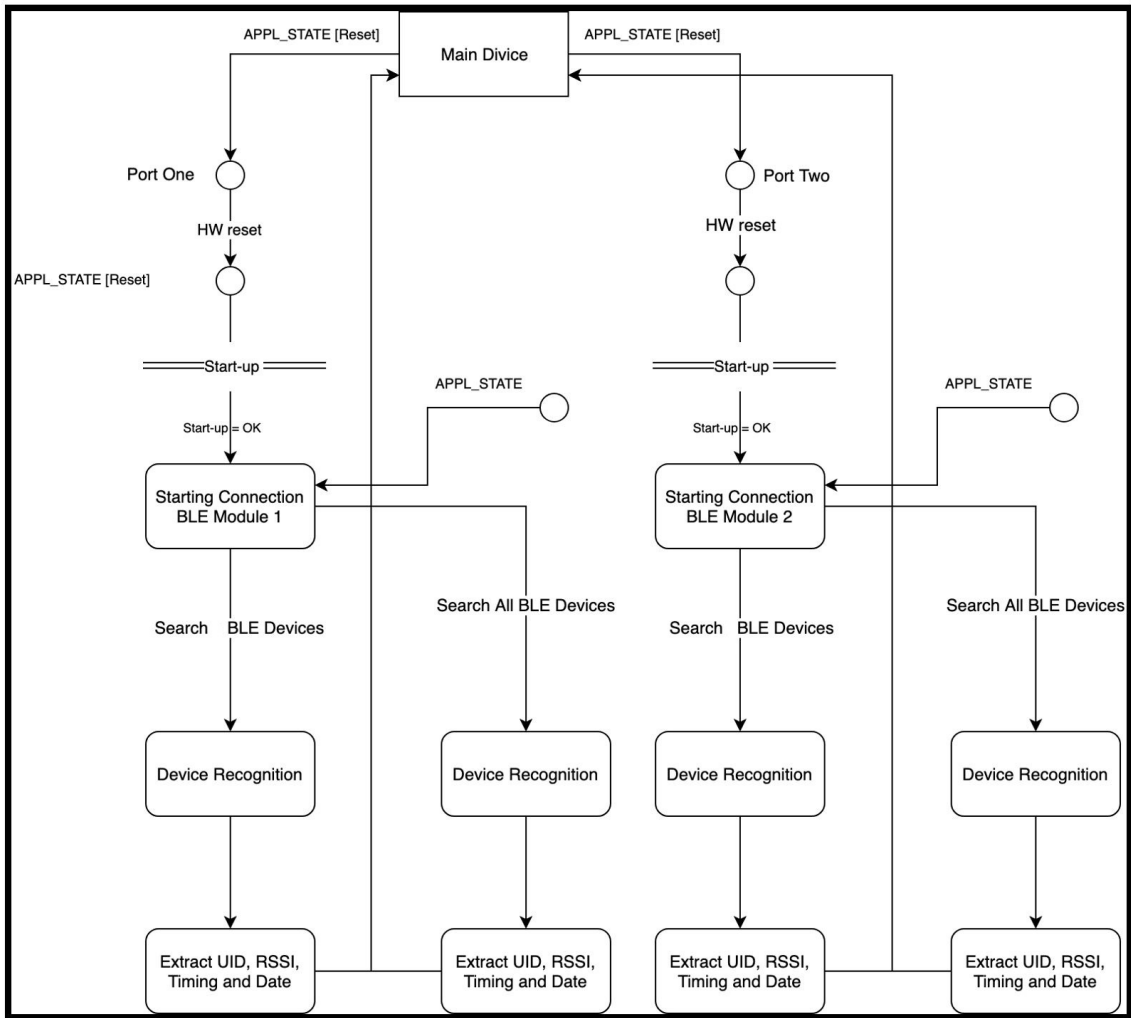
Figure 3.1: Block Diagram of LBS's platform for collecting RSSI measurements.

and comparisons are provided in Section 3.2. Finally, Section 3.3 concludes the chapter.

3.1 Fusion Framework

As shown in Fig. 3.1, the proposed fusion framework consists of a K-Nearest Neighbor (K-NN) fingerprinting module, which is used to construct (through a training phase) the RSSI map of the selected venue, and a PF-based state estimation module, which sequentially provides location estimates. More specifically, in the K-NN step, the venue is divided into N_{Zone} number of fingerprinting zones, where zone l, for ($1 \leq l \leq N_{\text{Zone}}$), is defined based on its geometric coordinates. The K-NN

step has the following two phases:

(i) An offline phase, where training database of the smoothed RSSI values is created from N_b sensors resulting in the training model in terms of the following RSSI vector

$$\text{Trained RSSI Set: } \{(\boldsymbol{\mu}_{\text{RSSI}}^{(1)}, \boldsymbol{\sigma}_{\text{RSSI}}^{(1)}), \ldots, (\boldsymbol{\mu}_{\text{RSSI}}^{(N_{\text{Zone}})}, \boldsymbol{\sigma}_{\text{RSSI}}^{(N_{\text{Zone}})})\}. \tag{3.1}$$

(ii) The online phase, where the RSSI vector of a real time user is measured and then compared with the pre-recorded training RSSI set (Eq. (3.1)) to estimate the zone of user's location. For finding the best match corresponding to the user's zone, K-NN classifier is used providing as output the label (center coordinates) associated with the user's zone together with its associated terms from Eq. (3.1). In other words, the output of the K-NN step is the centre coordinate $(X^{(l)}, Y^{(l)})$ of the predicted zone, where the target is expected, and its associated RSSI set, i.e.,

$$\boldsymbol{\mu}_{\text{RSSI}}^{(l)} = [\mu_{\text{RSSI}}^{(l,1)}, \ldots, \mu_{\text{RSSI}}^{(l,N_b)}]^T,$$
$$\text{and} \quad \boldsymbol{\sigma}_{\text{RSSI}}^{(l)} = [\sigma_{\text{RSSI}}^{(l,1)}, \ldots, \sigma_{\text{RSSI}}^{(l,N_b)}]^T, \tag{3.2}$$

where T denotes transpose operator.

The PF uses the coordinates $(X^{(l)}, Y^{(l)})$ corresponding to the centre of the predicted zone to perform the prediction step. In other words, first we oversample $N_p + M$ number of particles from the proposal distribution, i.e.,

$$\{\mathbb{X}_k^i\}_{i=1}^{N_p+M} \sim P(\boldsymbol{x}_k|\boldsymbol{x}_{k-1}). \tag{3.3}$$

Then, only N_p number of particles are selected such that they are limited to the zone $(X^{(l)}, Y^{(l)})$ specified by the communicated coordinates form the K-NN module. As the transitional density is used as the proposal distribution, the weights of the particles are updated as follows

$$W_k^i \propto W_{k-1}^i P(\boldsymbol{z}_k|\mathbb{X}_k^i). \tag{3.4}$$

In the update step based on Eq. (3.4), instead of forming the likelihood $P(\boldsymbol{z}_k|\mathbb{X}_k^i)$ based on each particle, we compute the probability that the measured RSSI for each sensor belongs to the variables (Eq. (3.2)) identified by the K-NN module. In other words, for calculating the likelihood, instead of considering just one RSSI value, a domain of RSSI values in a specific zone (e.g., zone l, for $(1 \leq l \leq N_{\text{Zone}})$) is used, i.e.,

$$W_k^i \propto P\big(\boldsymbol{\mu}_{\text{RSSI}}^{(l)} - 3\boldsymbol{\sigma}_{\text{RSSI}}^{(l)} \leq \boldsymbol{z}_k \leq \boldsymbol{\mu}_{\text{RSSI}}^{(l)} + 3\boldsymbol{\sigma}_{\text{RSSI}}^{(l)}|\boldsymbol{x}_k\big). \tag{3.5}$$

This completes presentation of the proposed multiple-model BLE-based estimation framework. Next, we present our experimental results.

3.2   Experimental Analysis/Results

As stated previously, the RSSI values fluctuate over time due to interference, path-loss, and other parameters that are yet to be identified. To classify the proximity of a user to a BLE device, it is essential to investigate parameters that potentially have high impact on the RSSI values. In this Section, first we empirically investigate, test, and compare effects of different parameters on the RSSI values, then we provide tracking results based on the proposed multiple-model BLE-based estimation framework.

3.2.1   Location-based Services Platform

Implemented LBS's platform for data collection is designed to gather different attributes of received BLE signals synchronously based on BLE module boards running BLE 4.2. The first step of the implementation is to set proper commands to gather raw data from activated BLE sensors. The raw database includes RSSI values obtained from different devices, Unique Identifiers (UID), and timestamps corresponding to the process of receiving different RSSI values.

A command line in Python 3.7 is coded to make a connection between the FC and the BLE modules through the available serial ports. The code is written in such a way that different BLE modules connected to the FC can be used synchronously to gather different information of the
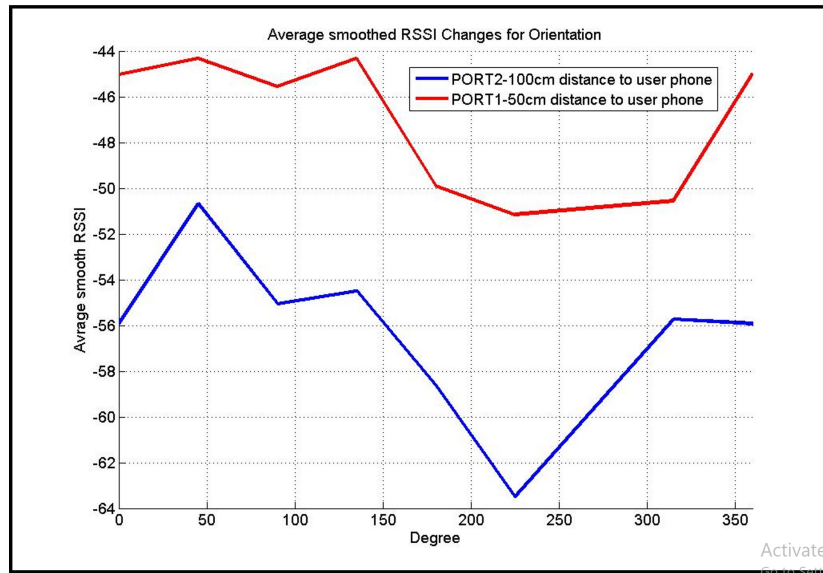
Figure 3.2: Orientation effect on the RSSI values.

devices. The devices, as peripheral in the advertising state, broadcast BLE advertising packets. The implemented software structure first makes a connection between the FC and different BLE modules simultaneously, and then sends request commands to the modules and asks them to gather different BLE advertisement packets. Received packets from the active modules are then sent to the tracking module implemented at the FC to be stored, processed, and plotted simultaneously. These extracted data including measured RSSI values and their related UIDs, date and timestamps from different ports connected to each module are sorted to be used in the proceeding processing steps. To focus on potential factors affecting the RSSI values, data collection is performed based on two different types of devices: At one hand, we used devices with commercially provided BLE software. On the other hand, we used ordinary BLE devices advertising around. We use an iPhone 8 plus as our device advertising. During the initial experiments, two different BLE modules are used simultaneously to gather BLE advertisement packets. Then the received raw data are processed and the related data (device UID, RSSI, date, and timestamp) are forwarded to the tracking module.

3.2.2 Effects of Different Parameters on RSSI Values

Evaluation of the effects of different parameters on the RSSI values is of great importance. In each experiment, we changed one parameter (e.g., orientation and distance to the beacon to
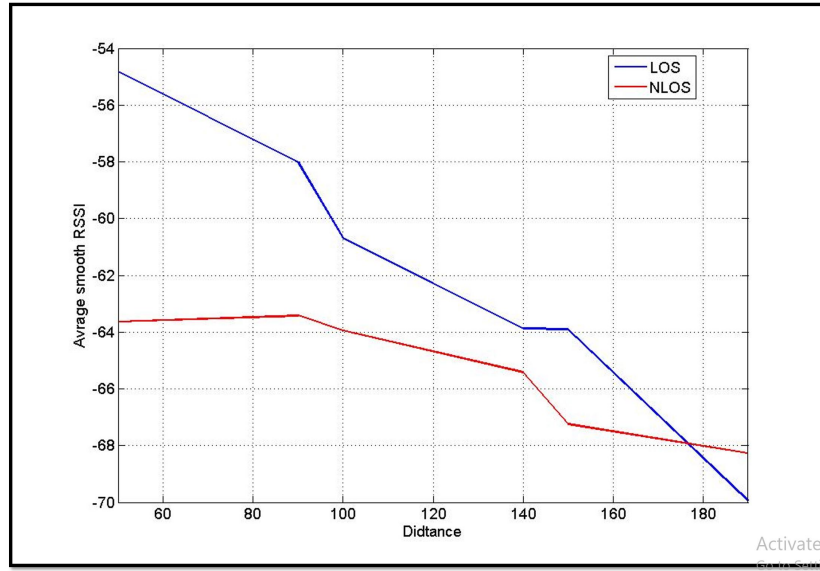
Figure 3.3: The RSSI values in case of LOS and NLOS condition.

name a couple), while the remaining parameters were fixed. Effect of the following parameters are investigated:

1. **User's Orientation**: To investigate and learn the potential relationship between user's orientation and the recorded RSSI values, two BLE modules are fixed with distance interval of 50cm. A mobile device is located at stable distances of 50cm and 100cm from the BLE Module 1 (referred to as Port 1) and BLE Module 2 (referred to as Port 2), respectively. Different orientations to the two sensing modules are tested, where at each orientation, 200 RSSI values from each of the two beacons are recorded simultaneously. Collected RSSI values are refined based on the smoothing mechanism presented in Section 2.1.1, and averaged at each orientation for evaluation purposes. Fig. 3.3 compares the transmitter's orientation effect on RSSI values for LOS and NLOS signal propagations.

2. **Line of Sight/ Non Line of Sight**: As is apparent, there is a relation between the RSSI values and distance via path loss model. In this experiment, D_0 is set to 50cm and RSSI values at distance 50cm are measured. Given this information, when distance D is known, then N can be calculated. To check effects of NLOS on the RSSI values, we considered the case where the BLE module is behind the user. For this aim, 200 RSSI values are measured, smoothed,
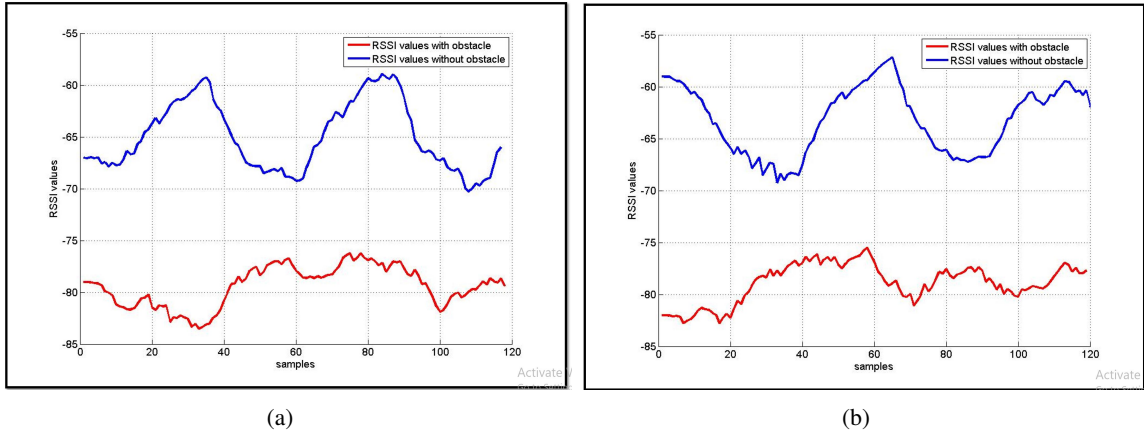
29

Figure 3.4: Wooden obstacle effect on two BLE module measurements. (a) RSSI values of BLE Module 1. (b) RSSI values of BLE Module 2.

and averaged at each distances ranging from $50cm$ to $190cm$ under two conditions, i.e., LOS and NLOS. As Fig.3.3 shows, the RSSI values under the NLOS condition are smaller than those associated with the LOS condition, therefore, the estimated distance computed based on pathloss model becomes larger than the actual distance.

3. **Presence of Obstacles in Environment**: As in a real world scenario, there would be obstacles between users and BLE modules. To investigate effects of such cases, we run this experiment measuring RSSI values with and without a wooden obstacle in the environment while the distance between the BLE module and the user is fixed. More specifically, we fix two BLE modules with distance interval of $150cm$ and measure RSSI values at the constant distance of $150cm$ to the middle point of two BLE connection line. Then measure 120 RSSI values under two conditions with and without the wooden obstacle. As can be observed from Figs. 3.4 (a) and (b), the RSSI values computed in presence of an obstacle are smaller than those collected in the absence of the obstacle.

The results and visions obtained from the above experiments provide insights for improving the achievable localization accuracy. This will be the focus of next section to improve the overall accuracy of the tracking framework by properly modeling and compensating the observed effects.
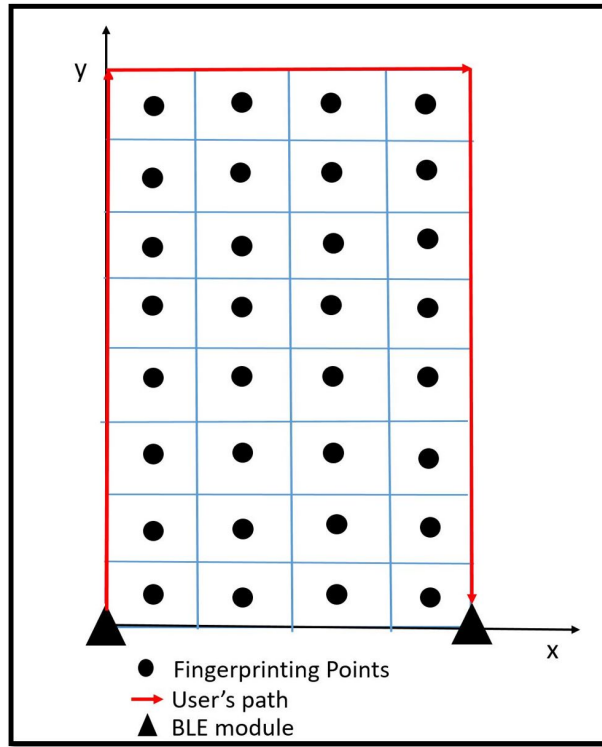
Figure 3.5: User tracking scenario for BLE-based indoor localization.

3.2.3 BLE-based Tracking Results

In this sub-section, we evaluate performance of the proposed tracking algorithm. For performing the tracking task, data collection is carried out in a 2m× 4m venue to experiment realistic situations close to a corridor environment. The venue is divided into 32 zones each with dimension of 50cm × 50cm. Total of 200 RSSI values are measured at the center of each zone. After smoothing and averaging the RSSI values, the fingerprinting data is formed. For testing, the user walks in a path around the venue as it is shows in Fig. 3.5.

First, K-NN algorithm is applied to find the zone where the user is located. After finding the zone of the user (zone's label), the PF uses the required information to form the overall estimate of the location of the target. The Mean Squared Error (MSE) is calculated as the criteria for evaluating the proposed multiple-model framework. Fig. 3.6 illustrates the calculated MSE values over varying number of particles. It can be observed that the proposed approach has the capability to provide near-optimal estimation results with increasing the number of particles to an acceptable range.
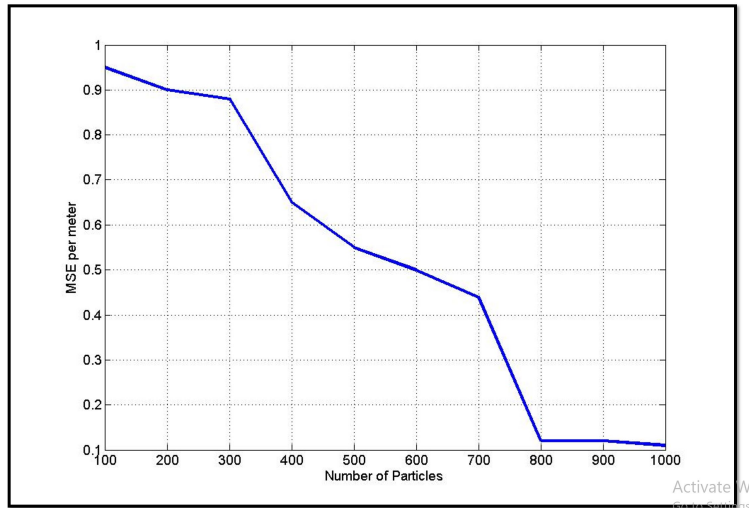
31

Figure 3.6: MSE computation as a function of number of particles (N).

3.3   Summary

Recent developments and advancements in signal processing, information fusion, communication, networking, and cloud technologies have resulted in the widespread emergence of the promising paradigm of the IoT. A key objective within IoT context is development of advanced signal processing and machine learning solutions to micro-locate and track a person within a delimited physical space (e.g. building) using BLE locating infrastructure installed within that space. Before achieving that ultimate goal, we performed an initial experimental phase where the goal was to test and validate effects of different parameters on the RSSI values. A fusion framework is then introduced by combining PF with K-NN algorithm. Based on real experiments performed through the implemented LBS platform, the proposed multiple-model fusion achieved acceptable results.

Chapter 4

Orientation-Matched Multiple Modeling for RSSI-based Indoor Localization via BLE Sensors

As discussed in Chapter 3, BLE-based localization is, typically, performed based on RSSI value, which suffers from different drawbacks due to its significant fluctuations. As analyzed in Chapter 3, orientation effects on RSSI values can be considered as a source of noise, reducing the localization accuracy. More specifically, the RSSI received from a smartphone in a fixed distance to the BLE receiver is subject to change when the orientation of the smart phone changes. In other words, the orientation of the transmitter of BLE packets to its receiver is considered as one of the most important parameters influencing the RSSI values. This chapter of the thesis, therefore, proposes a MM based fusion framework [72] that enhances the accuracy of the received signals and compensates the effects of orientation on the RSSI values. The proposed method highlights the importance of using inertial measurement units of smart phone and taking advantage of the phone's built-in sensors in the LBSs. The fusion of RSSI and IMU data [32, 73] would enhance the overall localization accuracy and mitigates the error caused by orientation of the BLE transmitter.

The reminder of the chapter is organized as follows: Section 4.1 presents the proposed orientation detection and MM framework. Section 4.2 presents the dataset and experimental settings and

the achieved results. Finally, Section 4.3 concludes the chapter.

4.1 Orientation Detection and RSSI Multiple-Modeling

We consider localizing a single target within the surveillance region monitored with N_b number of BLE-enabled senors. The RSSI value $Z^{(j)}$ associated with the jth active BLE sensor, for ($1 \leq j \leq N_b$), at each iteration is models as follows

$$Z^{(j)} = -10 \, N \, \log(\frac{D^{(j)}}{D_0}) + C_0 + v^{(j)}, \tag{4.1}$$

where $D^{(j)} = \sqrt{(X - X^{(j)})^2 + (Y - Y^{(j)})^2}$, and D_0 is the reference distance; C_0 is the average RSSI value at reference distance; $(X^{(j)}, Y^{(j)})$ denotes location of the jth BLE sensor, and; N is the path-loss exponent.

Orientation Classification via RSSIs: For finding the orientation of the user's phone, first a set of N_P RSSI values $\mathbb{X}_i = \{\text{RSSI}_i^{(j)}\}_{j=1}^{N_p}$ received by N_b BLE modules are measured in N_o different orientations ($\{\mathbb{X}_i^{(1)}, \ldots, \mathbb{X}_i^{(N_o)}\}$, for ($1 \leq i \leq N_b$). We have collected about $N_p = 10$ million RSSI values to be analyzed. The scenario that was chosen for collection of this dataset is to collect about 5 million RSSI values in 2 distances (1m and 3m). In each distance, we placed the user's phone in $N_o = 8$ different orientations and in each orientation $500,000$ RSSI values were collected. This large amount of data can provide us with invaluable dataset to be analyzed, smoothed and used to develop data-driven models.

As stated previously, RSSI values received from BLE beacons are prone to random and drastic fluctuations, which could result in inaccurate distance estimates. To prevent erroneous localization, a recursive Bayesian filter is used where a KF smoothing module is applied on each $\mathbb{X}_i$ to mitigate the RSSI fluctuations [74]. After smoothing RSSI values, different N_o-class classification algorithm including Support Vector Machine (SVM), K-NN, and Neural Networks (NN) are used to classify the RSSI values corresponding to each orientation. For orientation detection, the following two scenarios are considered:

(i) *Stand-alone Orientation Prediction*: In this scenario, RSSI values reported by just one BLE
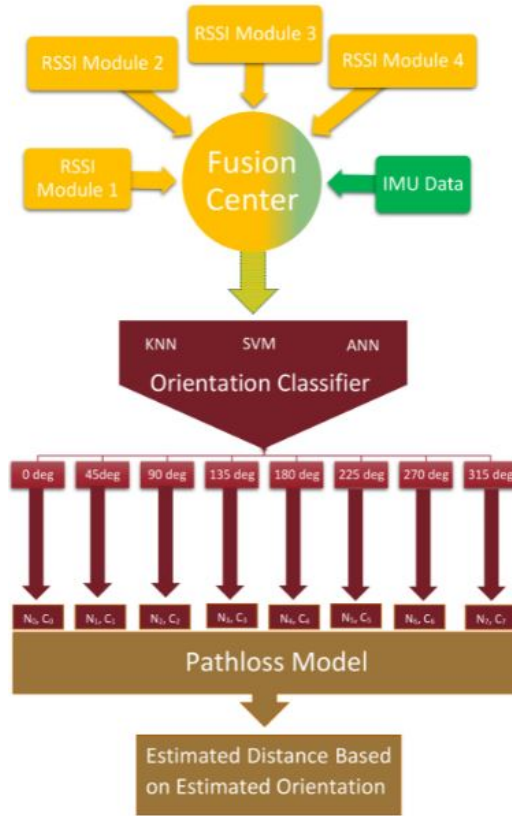
Figure 4.1: Block Diagram of the orientation-matched MM framework.

sensor are used as input to the classifier, therefore, we train N_b number of classifiers. In other words, each BLE sensor will provide us with 1-D label vector representing the orientation of the phone to that specific module.

(ii) *Multi-sensor Orientation Prediction*: Orientation prediction is performed in this scenario by using all N_b active BLE beacons. In this case, a classifier is trained based on features of length N_b consisting of smoothed RSSI values obtained from N_b active BLE sensors. In brief, the output of the classifier in this scenario is a vector representing the orientation of the phone to each BLE sensor.

The output of the orientation classification step is an estimate of the device's orientation, which as shown in Fig. 4.1 will be used to select one of the N_o orientation-matched path-loss models. The latter is described next.

4.1.1 Multiple Modeling Framework

We constructed orientation-matched path-loss models by learning parameters $\{N_j^{(m)}, C_{0,j}^{(m)}\}$, corresponding to orientation m, for $(1 \leq m \leq N_o)$, and module j, for $(1 \leq j \leq N_b)$ using the mean of the smoothed RSSI values of module j and orientation m at two different distances (D_0, D). After finding the phone's orientation, orientation-matched parameters associated with that specific orientation are replaced in Eq. (4.1) and distance D to the BLE module is calculated as follows

$$Z_j^{(m)} = -10\, N_j^{(m)} \, \log(\frac{D}{D_0}) + C_{0,j}^{(m)}. \tag{4.2}$$

For each sensor and for each particular orientation of the device to the beacon, the parameters of path-loss model are different. Therefore, in Scenario (ii) the distance estimated by each beacon is calculated separately. This provides a distance estimation matrix consisting of N values for distance. Weighted average of the distance estimation matrix is considered as the final value for distance estimation. In other words, considering that the classifiers has provided us with $[W_1, \ldots, W_{(N_b)}]$ where W_i denotes the accuracy of orientation classification for a given BLE sensor. Basically, the accuracy of each beacon in estimating the corresponding orientation of the smart phone represents the confidence rate of the classifier to accurately estimate the true distance with regards to the orientation of the smartphone. Therefore, the estimated distance for each beacon is weighted based on this confidence rate. By such definition, the higher the accuracy of a beacon in estimating the orientation, the greater the weight of the estimated distance for that specific beacon, i.e.,

$$D = \sum_{i=1}^{N_b} \frac{W_i}{\sum_{j=1}^{j=N_b} W_j} \times d_i, \tag{4.3}$$

where d_i states the distance estimated by each BLE module and weighted averaging method is used to gain the final estimated distance of the user to BLE modules. In summary, based on the constructed BLE dataset, the proposed MM framework (as shown in Fig. 4.1) is constructed where each one of the constituent components is an orientation-matched model resulting in total of eight localized orientation models. The aforementioned multi-sensor and data-driven model is then implemented that estimates the orientation of a hand-held device with high accuracy.
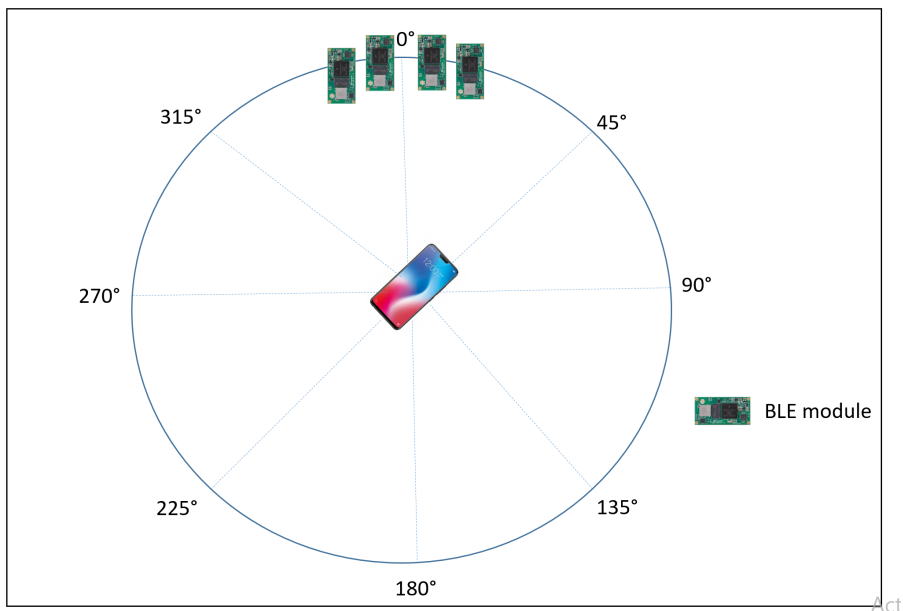
Figure 4.2: Real data collection setup for orientation detection.

4.2 Experimental Results

Real Data Collection Setup: As shown in Fig. 4.2, $N_b = 4$ BLE sensors are fixed in the same distance of $1m$ (for calculating the parameters of the orientation-matched path-loss models and $3m$ (for distance estimation) to the user's phone (IPhone 6). RSSI data is gathered for 8 orientations ($0°$, $45°$, $90°$, $135°$, $180°$, $225°$, $270°$, and $315°$) of user's phone to BLE modules. Moreover, all sensors are simultaneously gathering the IMU data for each orientation of the phone. The sampling frequency of RSSI values and IMU data is 16 samples per second. In order to prevent the effect of surrounding walls on collected RSSI value, the experimental environment is designed sufficiently far from any obstacle or wall in the vicinity of the sensors.

4.2.1 Stand-alone Classification-based on RSSI

Based on the mean of the smoothed RSSI values from $D_0 = 1$m and 3m, the orientation-matched path loss model parameters $\{N_j^{(m)}, C_{0,j}^{(m)}$ for ($j \in \{1, 2, 3, 4\}$), and $1 \leq m \leq 8$ are calculated for each sensor. Firstly, orientation estimation is performed with respect to the RSSI values

Table 4.1: Orientation classification accuracy comparison of the proposed algorithm for Scenario (i).

Approach Accuracy(%)			
Classification Method	**ANN**	**SVM**	**K(5)-NN**
BLE 1	**0.73**	0.70	0.65
BLE 2	0.68	0.62	**0.72**
BLE 3	0.66	0.69	**0.70**
BLE 4	0.66	0.69	**0.70**

Table 4.2: Orientation classification accuracy comparison of the proposed algorithms.

Approach Accuracy(%)			
Classification Method	Stand-alone RSSI	Stand-alone IMU	RSSI-IMU Fusion
ANN	70	90	97
SVM	72	93	96
KNN	74	92	99

received from each BLE module separately (Scenario (i)). In another attempt, the same orientation classification method is applied to the RSSI values received from all 4 modules simultaneously (Scenario (ii)). In both scenarios, 80% of all RSSI observations are considered as the training data and the remaining 20% RSSI observations are considered as the test data.

Table 4.1 illustrates the orientation classification accuracy for each BLE sensor for Scenario (i). The overall accuracy is not greatly satisfying as the RSSI value has drastic fluctuations causing misclassification of associated orientation. Consequently, based on the predicted orientations the distance of the smart phone to each BLE module is estimated using orientation-matched path-loss model. Compared to the conventional path loss models that estimate the distance with a fixed (N, C_0), the proposed method offers different parameters $(N_j^{(m)}, C_{0,j}^{(m)})$ for different orientations. It is worthy to mention that the same experiment was implemented for different distances between BLE sensors and smart phone and in most cases K-NN classifier gained the highest accuracy among all classifiers. The estimated distance for each BLE sensor is then compared to the real distance $(3m)$ and mean error of 1.69m, 1.57m, 1.19m, and 1.45m is recorded for Modules 1-4, respectively. Although the stand-alone approach based on Scenario (i) outperforms the traditional approaches in which one pre-defined (N, C_0) is considered for path-loss model, the difference is not significant.

To improve the overall accuracy of the orientation classification and mitigate the effects of RSSI fluctuations on orientation classification, Scenario (ii) is designed. In Scenario (ii), the weighted
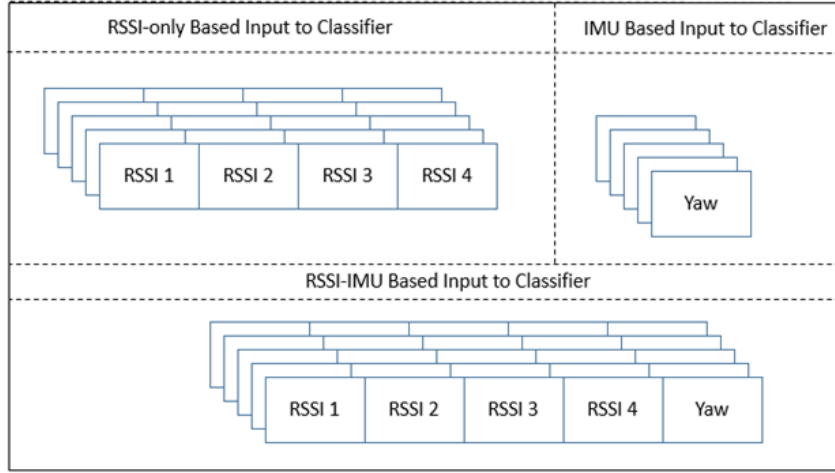
Figure 4.3: Schematic illustration of the input data for classification.

mean vector of 4 estimated distance vectors with weights proportional to the orientation prediction accuracy of the associated module $(0.73, 0.70, 0.72,$ and $0.64)$ is computed as the final distance vector using Eq. (4.3). The estimated distance vectors between phone to the 4 BLE modules is formed by mean error of 0.79m, 0.88m, 1.26m, 1.53m and weights $(0.73, 0.70, 0.72,$ and $0.64)$, respectively. The first column of Table 4.2 depicts the average accuracy of orientation classification in Scenario (ii). Comparing the average accuracy of Scenario (i) and (ii), it is observed that by considering RSSI values received from 4 beacons, one can estimate phone orientation with considerably higher accuracy. This improvement in Scenario (ii) highlights the efficiency of the proposed weighted averaging algorithm.

4.2.2 Stand-alone Classification-based on IMU

In the stand-alone approach based on IMU signals, the orientation classification of smartphone is implemented based on the IMU heading rather than RSSI values. As illustrated in Fig. 4.3, the IMU values are subject of classification. For this purpose, the same classifiers are used to classify the smart phone's heading into 8 different orientations ($0°$, $45°$, $90°$, $135°$, $180°$, $225°$, $270°$, and $315°$). Then based on each orientation associated to $(N_j^{(m)}, C_{0,j}^{(m)})$, the distance between smartphone and the BLE module is calculated. It is worthy to mention that for orientation classification purpose

just the IMU values are fed to the classification unit. Since IMU heading is more robust, it renders lower error in the distance estimation as shown in Table 4.2.

4.2.3 RSSI-IMU Fusion Classification

As for the RSSI-IMU fusion method, the vector consisting of the RSSI values and IMU values is subject of the classification. Therefore, the classifier has simultaneously the knowledge about the IMU sensors and the RSSI sensors resulting in a higher classification accuracy. In such a case,similar to the other two scenarios (stand-alone RSSI and stand-alone IMU classification) the distance is estimated based on the result of the orientation classification. Table 4.2 compares the classification accuracy of the three proposed methods. As is evident from the information provided in Table 4.2, the average classification accuracy of the fusion method is much higher. In the fusion method, however, the data of all 3 axis IMUs and BLE sensors should be collected simultaneously requiring more complexity in the data gathering phase. Furthermore, it is worthy to mention that the high classification accuracy obtained based on the fusion method resulted in lower distance estimation error of $0.71cm$, which highlights the importance of orientation of the smartphone for the localization task.

4.2.4 Discussions

A major issue is faced during the data collection process, i.e., RSSI values captured from different sensors in the same direction and similar situation act differently. In other words, the received RSSI values in some cases are radically different from others, which was an expected phenomena as sensor modules would not perform similarly. Based on this observed anomaly, we have two main categories of sensors (among the ones tested), where sensors in one category, more or less, perform similarly, while the other sensors act differently (higher average RSSI values at the same distance) but still close to each other. Another interesting observation is that in 135 degree and across different scenarios, there is a large decrease of the RSSI values in 1m. It was observed that the RSSI values collected at 1m with 135 degree are much lower than those obtained at 3m, which is an unexpected behavior. The conclusions discussed above are made based on several similar experimental analysis conducted over different distances and different orientations.

4.3 Summary

In this chapter, effects of a phone's orientation are investigated on the distance estimated by RSSI values. Since it is well known that variations occurring due to changes in orientation of a hand-held device is a limiting factor for BLE-based sensors, the inertial measurement unit data is also evaluated. In this regard, the chapter proposed an orientation detection and multiple-modeling framework to refine RSSI fluctuations by compensating the orientation effects. It is observed from the results of the proposed data-driven and orientation-free modeling framework that the location estimation is improved considerably when RSSI-IMU fusion model is implemented. The final error in distance estimation with combination of four BLE sensors is 0.72m. Without orientation considerations, the phone orientation can be any of ($0°$, $45°$, $90°$, $135°$, $180°$, $225°$, $270°$, $315°$) with mean error ranging as follows $1.69m$, $2.57m$, $2.19m$, $3.45m$. The error with orientation consideration of 0.72m is, therefore, less than minimum possible mean error without the orientation effect (1.69m).

Chapter 5

Online Dynamic Window Assisted Two-Stage LSTM Indoor Localization

As highlighted in Chapters 3 and 4, conventional IMU-based approaches, typically, use statistical and error prone heading and step length estimation techniques, preventing them to be used as practical, robust, real-time and accurate indoor positioning frameworks. In this regard, this chapter of the thesis takes one step forward to transfer offline IMU-based models to online positioning frameworks. More specifically, inspired by prominent advances in SP and NLP techniques, three near real-time dynamic windowing mechanisms are proposed based on a two stage LSTM localization architecture. The three underlying LSTM architectures are trained with 2100 AUs. Compared to the traditional LSTM-based positioning approaches suffering from either high tensor computation requirements or low accuracy preventing them for real-time deployment, the proposed ODW assisted two stage LSTM model can perform localization in a near-real time fashion. Performance evaluations based on a real PDR dataset shows that the proposed model can achieve exceptional classification accuracy of 92.4%, 96.4% and 94.3% for the three underlying LSTMs.

The remaining of the chapter is organized as follows: In Section 5.1, the conventional and the proposed DWs for implementation of near-RTLS two stage LSTM are represented. Experimental results based on prepared dataset are presented in Section 5.2 illustrating effectiveness and superiority of the proposed fusion based DW. Finally, Section 5.3 concludes the chapter.
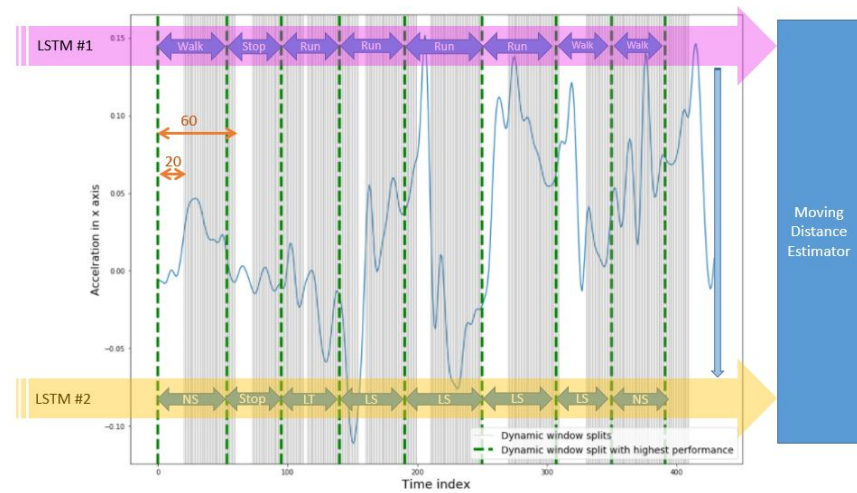
Figure 5.1: Diagram of the conventional two stage LSTM.

5.1 Proposed ODW assisted Two Stage LSTM Architecture

The essence of IMU based Indoor localization is based on recursive plausible location estimation based on prior step coordinates. In fact, smoothed 3 axis accelerometer and gyroscope data form sequential time series. RNN with linear chin structure has been deployed to analyze time sequence data in various domains (i.e., automation, NLP, speech recognition, image captioning and handwriting recognition). Despite the numerous accomplishments made by RNN networks, throughout the contemporary research works the limited capacity of contextual information and inability to back propagate in time has been reported as the downfalls of such networks. Since RNN consists iterative processing of the data segments, such networks and its variants are prone to vanishing and exploding gradient problems. LSTM is a type of artificial Recurrent Neural Network, deployed to address the aforementioned problems [21, 22, 70, 71]. A typical LSTM unit is consist if a memory cell, an input gate, an output gate, and a forget gate. The cell in LSTM is designed to process sequential segments of the data and maintains its hidden state through the course of learning. The implementation of cell assists LSTM network to overcome the challenges of traditional RNN during learning process. Recently there has been attempts to enhance the accuracy of indoor positioning using RNN, LSTM and its variants [21]. Great number of such systems utilize IMU of smartphone to measure bodily acceleration and angular velocity associated with different AUs. As

43

depicted in Fig. 5.1, such systems includes two LSTM classifiers and a moving distance estimator. While the first LSTM classifies the user's movement state (i.e., stop walking, running), the second one is designed to recognizing the AUs performed by the user (i.e., left and right turn, Short Step (SS), Normal Step (NS) and Long Step (LS), abnormal activity). The accelerometer and gyroscope readings representing bodily acceleration and angular movements of the subject in Cartesian coordinates respectively have drastic fluctuations in a sample course of time, resulting in inaccurate and misled classification model on AUs.

As an initial step for LSTM positioning, by utilizing a moving average filter on the sequential raw data reported from IMU sensors, one can remove or at least mitigate the fluctuation in the raw signal. In brief, the filter would average out the fluctuations or noisy patterns to obtain desired noise free sequential signal of IMU sensors. Having the raw data applied to a Low Pass Filter (LPF) or a moving average filter, the smoothed IMU data is then labeled empirically in an offline phase. The labeled 6 axis inertial data (consisting 3 axis accelerometer and 3 axis gyroscope data) is then fed to the LSTM network as training data. It is worthy to mention that once the smoothed inertial data is derived, the training and test segments of data are splitted in an offline phase using a dynamic window given by

$$
A \;=\; \begin{pmatrix} S_1(x_f^a(n+L) \\ S_2(x_f^a(n+L) \\ \vdots \\ S_i(x_f^a(n+L) \end{pmatrix} (20 \le L \le 60), \tag{5.1}
$$

where $S_i(x_f^a(n+L)$ represents i^{th} segment of the filtered inertial signal. The segmented inertial sensor data reported by IMU sensors carry sufficient information about the bodily acceleration and angular velocity patterns of different AUs and movements performed by the user during path trajectory. Different data segments along with the empirically derived labels will be sequentially fed to LSTM networks, which classify the segments into different movement states (i.e., running, walking, stopping) and different AUs (i.e., left and right turn, SS, NS and LS and abnormal activity). The

challenge preventing the algorithm to be identified as a real-time localization is a dynamic window, which excessively splits the sequential data into great number of data segments, as the input to LSTM networks in an offline phase. The algorithm would then choose the most viable segment based on the best recognition performance.

The implementation principle of moving distance estimator is similar to PDR, although in the proposed two stage LSTM, the current location of the user updates based on each recognized activity and its related AU rather than heading and statistical stride length estimation. The moving distance estimator is given by $P_k = P_k - 1 + A\amalg_k$, where k shows the current time index of the position (P) and the recognized action unit ($A\amalg_k$). The step length of the participants using the mode length value of step type recognized by LSTM (e.g., SS, NS, or LS) can be determined as follows

$$A\amalg_k = \Psi_k, \tag{5.2}$$

$$\Psi_k = \Pi(\gamma_k, \lambda_k, \delta_k) \tag{5.3}$$

$$\text{and} \quad \Psi_k = \Gamma(k), \tag{5.4}$$

where Ψ_k is the assumed step length, and Π is the function mapping each subject (γ_k) with the mode of step length ($\Gamma(k)$) of the particular step length type (λ_k) according to type of activity (δ_k) performed in the current time index (k). Once the most viable segment based on the best performance of the recognition model is chosen, then the next segment is fed to LSTM network. The implementation of excessive tensor computation is not efficient in terms of time, memory and computation power. The conventional dynamic window for two stage LSTM indoor positioning does not satisfy the RTLS requirements. Although the algorithm yields high accuracy of AU classification, the dynamic window slides through the test data in an offline phase, requiring excessive computation for each AU recognition. Even if implemented in semi real-time running manner, there is lack of processing power to deal with high requirement s of tensor computation and AU recognition. In this article the goal is to address the aforementioned challenges by proposing three different (SP, NLP and SP-NLP based) ODWs.
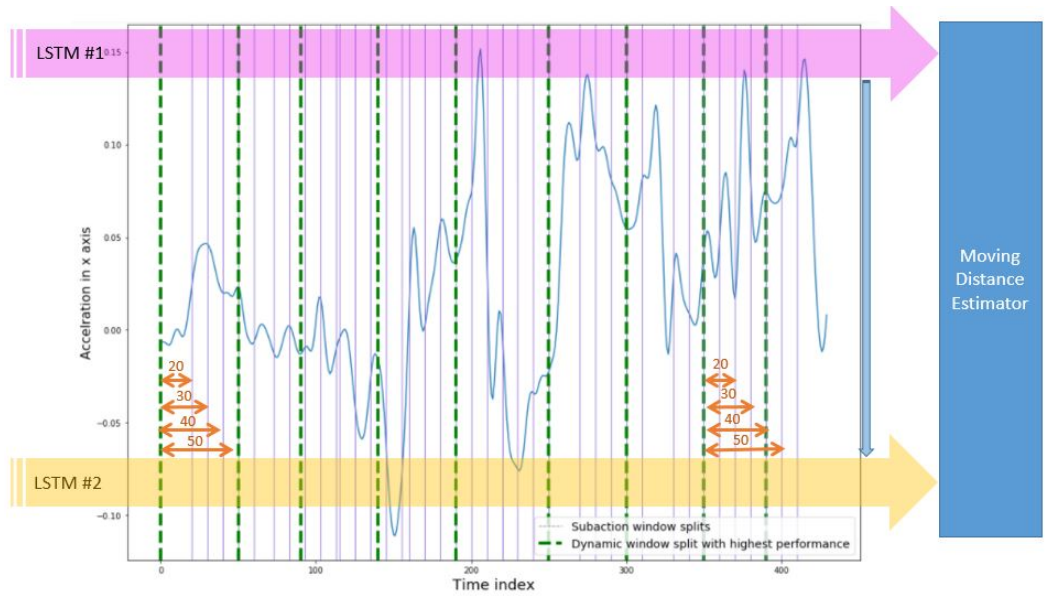
Figure 5.2: NLP inspired online dynamic window.

5.1.1 NLP inspired Dynamic Window

Inspired by ubiquitous implementation of NLP techniques in various domains of AI, a solution for near real-time implementation of two stage LSTM is proposed. Considering conspicuous similarities between sequential IMU and text data, we can model the positioning problem in terms of NLP model. In state-of-the-art NLP classification solutions, the algorithms can be trained based on multivariate sentences as input data types. Once trained, these frameworks can perform classification on multivariate sequential data in the test phase. In fact, in order to process the real time sequential data collected from iOS-based SDK, the LSTM models should be trained on multivariate data stored in the database (Fig. 5.3) for each AU in the database. In other words, although the patterns of the data for each AU are highly correlated, the length of that action unit can vary based on physical parameters of the user's body, frequency of steps taken by the user and the gait cycle information of pedestrian. The "multivariate" term in sequential data refers to the non-uniformly splitted subsets of time series sequential data in this research work. In fact, a typical statement is consist of several sentences, each of which includes different number of words. In order for the algorithms to be trained on the multivariate data a practical technique is deployed to turn meaningful pieces of data (such as words) into random string of characters or numbers called token that has
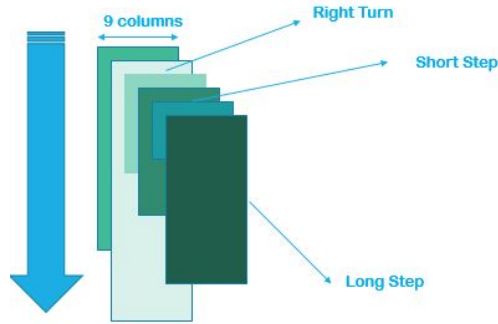
Figure 5.3: Multivariate AU data.

no meaningful value if breached. Therefore, the problem of training and testing multivariate data is resolved by tokenization technique. In fact, tokenization is considered as a key and mandatory aspect of working with text data in NLP applications.

Considering the aforementioned solution to resolve multivariate training of the NLP models, one can model IMU sequential readings to the statements in NLP. Additionally, deploying tokenization concept in AU classification, one can consider tokens as small subsets of an action performed by the user. Similar to NLP classification methods, where the tokenized words as subsets of a statement form a sequential meaningful statement, in this application uni-variate subsets of AUs form a meaningful action performed by the user. Implementation of such method prevents excessive tensor-based calculations and reinforces the performance of near real-time indoor tracking method. In other words, the proposed NLP-based dynamic window would split the test set into considerably fewer number of tensors. Consequently, the algorithm can assess the performance of LSTM network with different input lengths (multiplies of token length) and recognizes the user's AU. As is shown in Fig. 5.2, the NLP inspired DW can split the sequential test data with fewer number of segments, which reduces the computation requirement for the proposed framework.

5.1.2 Signal Processing Dynamic Window

An another solution to establish a near-RTLS framework, we attempt to analyse the signal pattern using the accurate step detection method developed in our last research work to split the test data
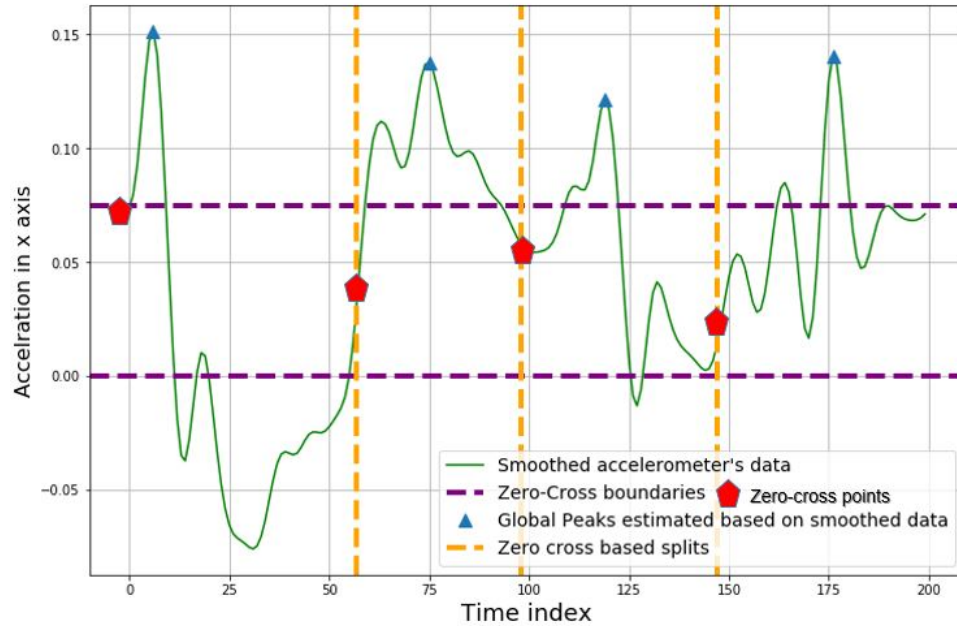
Figure 5.4: Signal Processing based online dynamic window.

based on the knowledge of the step indexes. As the accelerometer reports three axis inertial information of the smartphone movements, one can detect the step indexes of the signal using an accurate step detection algorithm. Once the step indexes are identified, the SP-DW searches for zero crossing points, representing the starting and ending points of each performed AU. Each zero crossing point should abide all of the following rules to be picked as starting/end index of an AU. First of all each zero-cross point should be between two consecutive peak points. Moreover, each zero point should be in zero-cross vicinity. In the normal walking mode, each zero cross point should be almost in the middle of two consecutive peaks. Additionally, there should not be two zero cross points between two consecutive peaks. The pedestrian steps are represented through the distinct peak patterns, as shown in Fig. 5.4 where the number of peaks indicate the total number of steps. Although SP-dynamic window is not able to accurately recognize the starting and end of AUs, the required computational delay in this method is less than both conventional and NLP-based DWs since its performance is not dependent on any tensor assessment. In other words, SP-dynamic window attempts to split the test data and recognizes the starting and end of each AU without trying to identify the action. Once the test data is splitted the AUs will be transformed to LSTM classifier to detect the corresponding label of each AU based on the signal pattern and deep extracted features

48

in model.

5.1.3 SP-NLP fusion Dynamic Window

Each SP and NLP method benefit from particular and different advantages in real-time implementations. The methodology of NLP based dynamic window is based on fewer number of tensor calculations and the assessment of LSTM model on multivariate test data while SP based dynamic window provides significantly faster test splitting techniques. In fact, in real time scenarios SP based dynamic window renders higher localization speed with lower accuracy while NLP takes advantage of multiple tensor assessments prior to AU classification. Such differences in performance of real-time scenarios led to deploy a fusion model referred to SP-NLP fusion dynamic window. The goal of implementation of such fusion model is to establish a trade off between accuracy and run time delay required in RTLS.

The methodology of the proposed framework consists two phases:

(1) **SP-DW**: First the SP framework would detect the peaks and eligible step indexes in the sequential preprocessed signal reported by IMU sensors. Based on the peaks and rule based zero cross vicinity, the zero cross points in sequential data would be detected. By determining the zero cross indexes, the sequential data can be splitted into segments while segments are the inputs to LSTM classifiers. If the accuracy of LSTM classification exceeds a defined threshold, the segment would be picked as an AU. Otherwise NLP-DW would be used to segment the AU in a more accurate fashion. The algorithm evaluates the accuracy of SP-DW segments (Υ), with regards to a predefined threshold τ_1. Then the framework would either implement the localization based on SP-DWs or pass the sequential signal to NLP-DW for re-segmentation.

(2) **NLP-DW**: If the segments splitted by SP-DW does not exceed the threshold, an NLP based model would receive the knowledge of the zero crossing indexes in the sequential data and attempts to find the nearest k neighbor tokens of the step index. Consequently, $k + 1$ tensors would be fed to LSTM to recognize the AUs and their corresponding labels. Finally, the segment with highest performance metric (i.e., accuracy) represents the AU. The overall decision
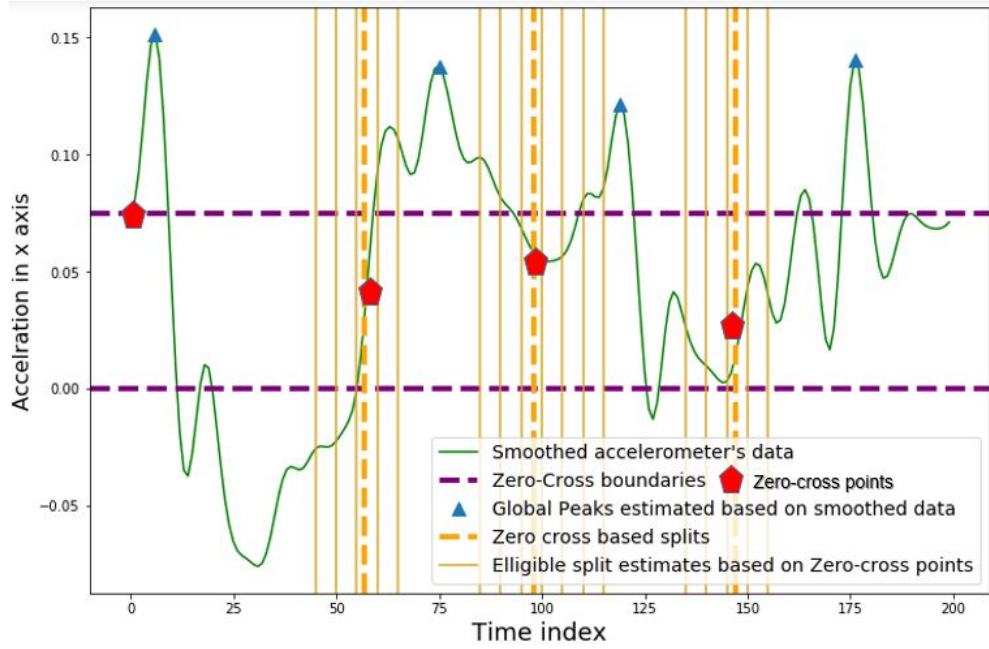
Figure 5.5: SP-NLP based online dynamic window.

algorithm for the proposed algorithm is given by

$$
\Upsilon = \begin{cases} \Upsilon \geq \tau_1 \longrightarrow \text{Localization} \\ \\ \Upsilon \leq \tau_1 \longrightarrow \text{NLP-DW} \begin{cases} \eta \geq \tau_2 \longrightarrow \text{Localization} \\ \eta \leq \tau_2 \longrightarrow \text{No valid AU} \end{cases} \end{cases}
$$

As expected, the accuracy of SP-NLP dynamic window is higher than the two other proposed methods (i.e., SP and NLP based DWs) since it simultaneously benefits from not only the zero crossing indexes but also the tensor calculation. Moreover, in SP-NLP dynamic window, as the tensors are chosen based on zero crossing knowledge the probability of correct AU recognition would be higher. Furthermore, compared to NLP based dynamic window, the SP-NLP model would recognize the AUs much faster than proposed and conventional models. Fig. 5.5 represents the segments in SP-NLP based online dynamic windowing approach.
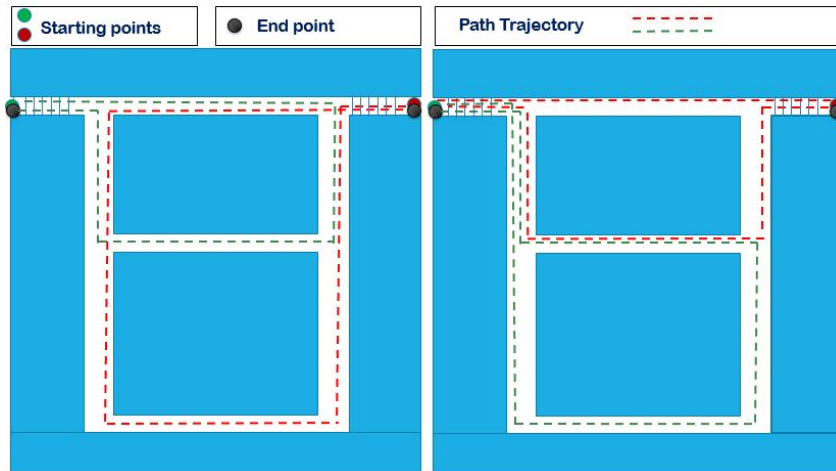
50

Figure 5.6: Path Trajectories designed for ODW assisted two stage LSTM approach.

5.2 Simulation Results

To evaluate the real-time implementation of NLP-inspired and SP-based dynamic windows, an experiment protocol is designed prior to data gathering phase. The data used in this research work is consist of data set collected by Ghulam Hussain et al in 2019 [21] and the newly collected data using our developed iOS application and iPhone 11 pro IMU sensors for more comprehensive investigation. In the newly designed data gathering setup, total number of 80 inertial data sets were collected by two different users in 4 distinctive path trajectories illustrated in Fig. 5.6. Each user can follow the pre-defined path trajectories by their own choice. Based on the predefined instructions, in half of the test data sets (40 tests) the user holds the smart phones by their right hand and the rest of the data was collected while the user holds the smart phone by left hand. To be aligned with the conventional data set the sampling frequency was fixed (50Hz). The inertial raw data collected (Comma-Separated Values (CSV)) files in the smartphone is propagated to the back-end server using a smartphone SDK. As in real time scenarios, the movement statuses are not confined to stop walking and running, the newly designed path trajectories consist two more movement statements of upstairs and downstairs to further enhance the indoor localization technique. The corresponding AU label to each time segment is reported by actively monitoring pedestrian trajectory using cameras installed in the venue. In this experiment, 7 AUs (Long Step (LS), Normal Step (NS), Short
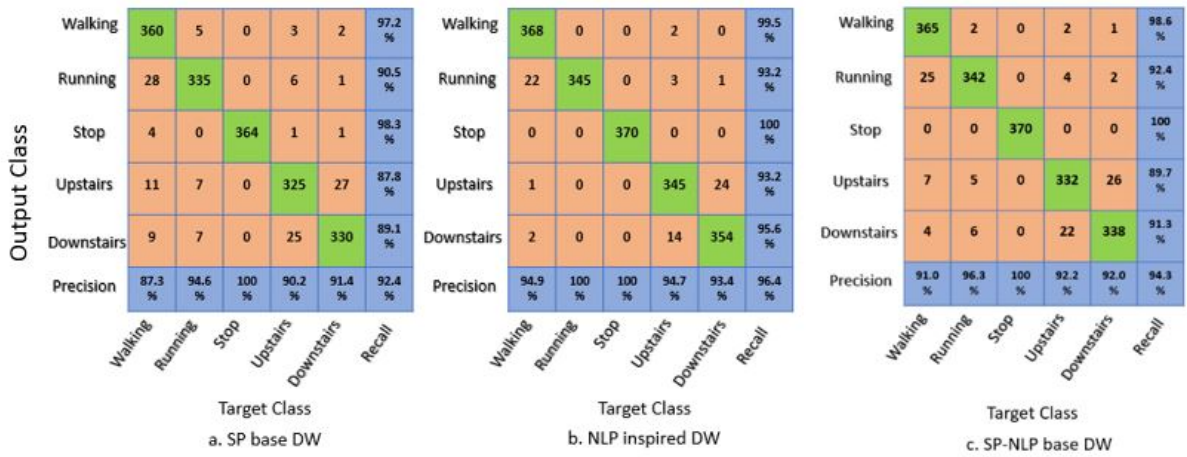
Figure 5.7: Confusion matrix comparison of different DWs representing the LSTM performance for Movement status recognition (test accuracy)
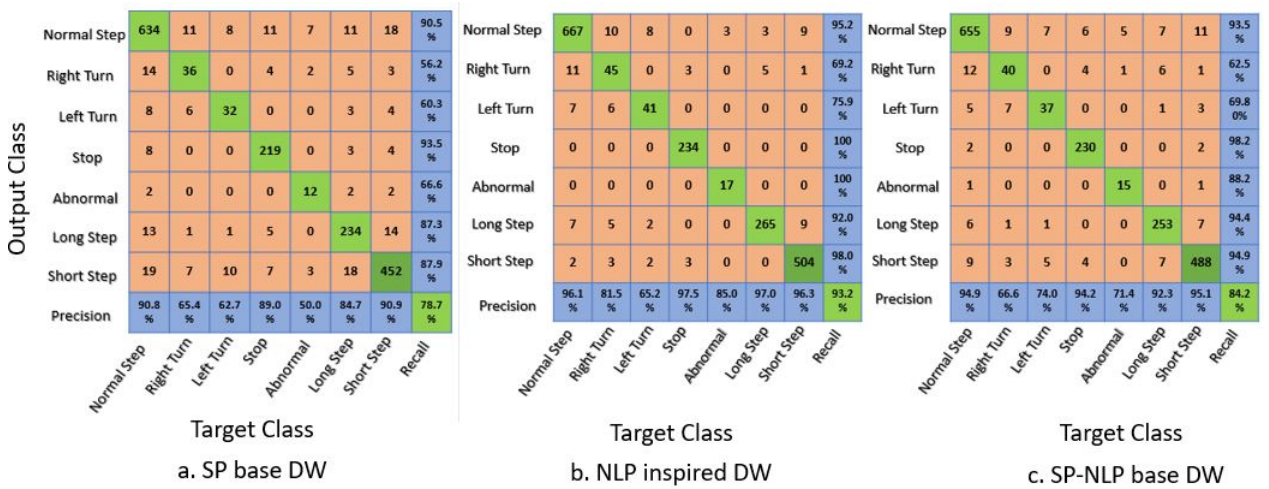
Figure 5.8: Confusion matrix comparison of different DWs representing the LSTM performance for AU recognition (test accuracy)

Step (SS), Left Turn, Right Turn, Abnormal, Stop) and 5 moving states (Walking, Running, Stop, Down Stairs, Upstairs) are considered for LSTM classifications. The LSTMs were trained over the data on conventional research work as well as the newly collected data after initialization of hyper parameters. Once the LSTM networks are trained, the implementation of different proposed dynamic windows can be evaluated on the test set. Despite the conventional LSTM based positioning systems, the test set in this chapter is not splitted into AU in a passively in an offline manner. In contrast to contemporary LSTM approaches, in this implementation, the algorithm receives the

Table 5.1: Run time and average accuracy comparison of ODW assisted two stage LSTM based indoor localization

Parameter		Traditional Dynamic Window	SP based Dynamic Window	NLP inspired Dynamic window
Number of tensor calculations		280	0	15
Average running delay (per AU)		30 sec	0.5 sec	2.6 sec
Average Accuracy	LSTM#1	97.9%	78.6%	88.6%
	LSTM#2	95.9%	70.4%	82.3%

test set of data simultaneously as the user walks through path trajectory in the venue. Assisted by proposed dynamic windows, the methods attempt to split the test data stream into eligible subsets representing AUs. Table 5.1 provides the run time and average accuracy comparison of ODW assisted two stage LSTM based indoor localization. As expected, the required time to process an AU in proposed methods (SP-DW and NLP-DW) are considerably less than the conventional model. More importantly, the accuracy of AU and moving state classification (LSTM 1 and LSTM 2) remained respectively high. NLP model is more accurate in positioning since the distance in such model is obtained from high tensor computations whereas in NLP inspired DW model, an average error of $0.934\,\mathrm{m}$ in an indoor area of $131.5\,\mathrm{m}^2$ was measured. The confusion matrix comparison of conventional, SP based and NLP inspired DWs are reported in Figs. 5.7 and 5.8 .

5.3   Summary

Inspired by ubiquitous advances in sequential data processing, in this chapter three ODW assisted two stage LSTM models are implemented. In first attempt NLP inspired DW is introduced which could significantly reduce the computation time required for indoor positioning. In another attempt to analyze the IMU sequential signal, SP-DW was implemented which could further decrease the processing time for two stage LSTM based indoor localization. While accuracy of $1.5m$ and $1.1m$ were obtained for near real time SP and NLP inspired DWs, the proposed methods outperform the conventional framework where the implementation of near real time system was impossible. Finally in order to end up with a trade of between the accuracy and running time of the proposed algorithms, SP-NLP based ODW is proposed.

Chapter 6

Summary and Future Research Directions

This chapter concludes the thesis with a list of important contributions made in this dissertation. In addition, potential directions for future research will be outlined.

6.1 Summary of Thesis Contributions

The research works performed in this thesis are motivated by recent advancements and developments of autonomous multi-agent systems. Such applications require the network to be able to identify, track, and monitor intelligent agents in an indoor environment and perform conditional tasks with minimum human intervention. Current commercial indoor localization approaches are based on different indoor localization technologies, including IR, US systems, RFID, ZigBee, WiFi, BLE, UWB, and Optical-based frameworks. The focus of the thesis is on identifying and addressing the challenges of BLE-based positioning and enhancing its accuracy by proposing IMU assisted MM frameworks. Moreover, in order to yield a scalable, efficient, and respectively accurate RTLS systems, three ODW assisted two-stage LSTM frameworks are proposed. In summary, the thesis made a number of contributions [20, 43, 44] as briefly outlined below:

(1) **Multiple Model BLE-based Tracking via Validation of RSSI Fluctuations under Different Conditions** [20]: In this work, effects of different parameters directly influencing RSSI

values in an indoor positioning system are evaluated. Furthermore, a multiple-model fusion framework is proposed by combining PF with K-NN algorithm to micro-locate and track a person within a delimited physical space (e.g., an office building) using BLE locating infrastructure installed within that space. Based on real experiments performed through the implemented LBS platform, the proposed multiple-model fusion framework achieved an increased overall accuracy. To be more specific, the proposed framework consists of the following two components:

- *Data Acquisition and Smoothing Module*: This is an initial experimental phase with the goal of testing and validating effects of different parameters on the RSSI values. Based on the validation results, a KF-based smoothing filter is developed with the objective of reducing the RSSI fluctuations.

- *Fusion Centre*: The second component is the tracking module, which is a fusion model developed by coupling PF with K-NN algorithm. The objective is to test and validate effects of different parameters on the tracking performance. In contrary to the conventional PF-based solutions that use RSSI measurements regardless of the environmental conditions (i.e., presence of obstacles in the environment), LOS/NLOS propagation, orientation of transmitter and receiver of the BLE packet, the proposed MM framework tests and validates the effects of different parameters on the RSSI values and on tracking performance.

(2) **Orientation-Matched Multiple Modeling for RSSI-based Indoor Localization via BLE Sensors** [43]: The thesis proposed an orientation detection and multiple-modeling framework to refine RSSI fluctuations by compensating the orientation effects. It is observed from the results of the proposed data-driven and orientation-free modeling framework that the location estimation is considerably improved when the proposed RSSI-IMU fusion model is implemented.

(3) **Online Dynamic Window Assisted two-stage LSTM for indoor positioning** [44]: The thesis proposed a novel online dynamic window assisted two-stage LSTM framework for near real-time localization based on distinctive IMU data patterns. The proposed framework

consists of two LSTM classifiers and a moving distance estimator. The first LSTM classifies the user's movement state (i.e., stop, walking, and running states) while the second LSTM model is designed to recognize the AUs performed by the user (i.e., left and right turn, short, normal and long step, and abnormal activity). The moving distance estimator updates the current location of the user based on each recognized activity and its associated AU. The proposed framework consists of the following two phases:

- *Offline Phase*: The IMU values for each AU and movement state is collected, smoothed via moving average filter, and labeled empirically using the video cameras installed in the venue.

- *Online Phase*: This phase consists of pattern matching and post-processing steps. In the online phase, the real-time sequential IMU data is measured, then a moving average filter is applied for two reasons: (i) To smooth fluctuations and sudden drifts in the IMU signals, and; (ii) To prepare the data for step, peak, and zero cross detection algorithms. The pre-processed sequential data would then be splitted using the proposed ODW methodologies (i.e., inspired by NLP and SP techniques).

6.2   Future Research

In what follows, potential future research directions are presented to further improve the frameworks proposed throughout the thesis:

(1) The proposed indoor localization frameworks have been evaluated based on real datasets collected via 4 and 5 BLE devices in a $6\,m \times 5\,m$ room. It would be interesting, as a direction for future works, to investigate performance of the proposed approaches in larger indoor environments with more Bluetooth devices.

(2) Another potential research direction is to explore if a hybrid solution can be developed by utilization of BLE devices and other infrastructures or different signaling technologies (e.g., WiFi and/or UWB) to help improve accuracy of RF-based indoor localization.

(3) In this thesis, a near real-time solution to indoor localization is proposed. Inspired by advances in sequential signal processing models, one can implement an RTLS framework that not only benefits from the RSSI values provided by BLE sensors but also takes advantage of portable embedded inertia data reported by IMU sensors. Such a framework would be scalable, efficient, cheap, and accurate.

(4) Extension of two-stage LSTM indoor localization approach can be a direction for the future research. The proposed IMU based indoor localization approach can be further improved by extending the two-stage LSTM framework to consider other embedded sensors in the smart phone such as lightening and barometer sensors.

(5) Recent research works have shown benefits of using high time-domain resolution based on the UWB technology, which enables accurate indoor localization/tracking. Existing UWB-based systems are, however, designed to localize an object in a small target venue with limited number of tags. Moreover, the UWB based indoor localization methods such as Time of Flight (TOF), Two Way Ranging (TWR), Time Difference of Arrival (TDOA) require either propagation of several messages between tag and anchor node or time synchronization between anchors, adding more complexity and computation to the method. Development of hybrid BLE and UWB technologies is a fruitful direction for future research.

References

[1] C. Xu, L. Yang and P. Zhang, "Practical Backscatter Communication Systems for Battery-Free Internet of Things: A Tutorial and Survey of Recent Research," *IEEE Signal Processing Magazine*, vol. 35, no. 5, pp. 16-27, Sept. 2018.

[2] S. Tarkoma and H. Ailisto, "The Internet of Things program: The finnish perspective," *IEEE Commun. Mag.*, vol. 51, no. 3, pp. 10-11, Mar. 2013.

[3] M. Z. Win, F. Meyer, Z. Liu, W. Dai, S. Bartoletti and A. Conti, "Efficient Multi-sensor Localization for the Internet of Things: Exploring a New Class of Scalable Localization Algorithms," *IEEE Signal Processing Magazine*, vol. 35, no. 5, pp. 153-167, Sept. 2018.

[4] 2. P. Spachos, I. Papapanagiotou and K.N. Plataniotis, "Microlocation for Smart Buildings in the Era of the Internet of Things: A Survey of Technologies, Techniques, and Approaches," *IEEE Signal Processing Magazine*, vol. 35, no. 5, pp. 140-152, Sept. 2018.

[5] C. Xu, Y. Sun, K.N. Plataniotis, N. Lane, "Editorial - Signal Processing and the Internet of Things," *IEEE Signal Processing Magazine*, Special Issue, vol. 35, no. 5, September 2018.

[6] U. Varshney, "Pervasive Healthcare Computing: EMR/EHR, Wireless and Health Monitoring," *Springer-Verlag*, 2009.

[7] F. Amirjavid, P. Spachos, K.N. Plataniotis, "3-D Object Localization in Smart Homes: A Distributed Sensor and Video Mining Approach," *IEEE Systems Journal*, vol. 12, no. 2, pp. 1307-1316, June 2018.

[8] X. Li, R. Lu, X. Liang, X. Shen, J. Chen, and X. Lin, "Smart Community: An Internet of Things Application," *IEEE Commun. Mag.*, vol. 49, no. 11, pp. 68-75, Nov. 2011.

[9] K. Zheng; H. Wang; H. Li; L. Lei; W. Xiang; J. Qiao; X. Shen, *IEEE Transactions on Vehicular Technology*, 2017.

[10] S. HassanHosseini, M. R. Taban, and J. Abouei, "Indoor localization of wireless emitter using direct position determination and particle swarm optimization," Turkish Journal of Electrical Engineering & Computer Sciences, vol.26, no. 2, pp. 655-665, Mar. 2018.

[11] S. HassanHosseini, M. R. Taban, J. Abouei, and A. Mohammadi, "Improving performance of indoor localization using compressive sensing and Normal Hedge algorithm," Turkish Journal of Electrical Engineering & Computer Sciences, vol. 28, no. 4, pp. 2143-2157, July 2020.

[12] A.Kushki, K.N. Plataniotis and A.N. Venetsanopoulos "WLAN positioning systems: principles and applications in location-based services" Cambridge University Press, 2012.

[13] P. Davidson; R. Piche, "A Survey of Selected Indoor Positioning Methods for Smartphones," in *IEEE Communications Surveys & Tutorials*, In Press, 2017.

[14] S. Sadowski and P. Spachos, "RSSI-Based Indoor Localization With the Internet of Things," *IEEE Access*, vol. 6, pp. 30149-30161, 2018.

[15] S. Kumar, R. Ramaswami and K. Tomar, "Localization in Wireless Sensor Networks using Directionally Information," *IEEE International Advance Computing Conference (IACC)*, 2013, pp. 577-582.

[16] F. Zafari, I. Papapanagiotou, M. Devetsikiotis, T.J. Hacker, "An iBeacon based Proximity and Indoor Localization System," https://arxiv.org/abs/1703.07876, 2017.

[17] C. Xu, Y. Sun, K.N. Plataniotis, N. Lane "Editorial - Signal Processing and the Internet of Things," *IEEE Signal Process. Magazine*, vol. 35, no. 5, 2018.

[18] P. Spachos, I. Papapanagiotou and K.N. Plataniotis, "Microlocation for Smart Buildings in the Era of the Internet of Things: A Survey of Technologies, Techniques, and Approaches," *IEEE Signal Process. Magazine*, vol. 35, no. 5, 2018.

[19] S. Mehryar, P. Malekzadeh, S. Mazuelas, P. Spachos, K. N. Plataniotis, and A. Mohammadi, "Belief condensation filtering for RSSI-based state estimation in indoor localization," IEEE International Conference on Acoustics, Speech and Signal Processing (ICASSP), May 2019, pp. 8385–8389.

[20] M. Atashi, M. Salimibeni, P. Malekzadeh, M. Barbulescu, K. N. Plataniotis and A. Mohammadi, "Multiple Model BLE-based Tracking via Validation of RSSI Fluctuations under Different Conditions," *2019 22th International Conference on Information Fusion (FUSION)*, ON, Canada, 2019, pp. 1-6.

[21] G. Hussain, ,M.S. Jabbar, ,J.-D. Cho, ,S. Bae, "Indoor Positioning System: A New Approach Based on LSTM and Two Stage Activity Classification." *Electronics*, 8, 375, 2019.

[22] Q. Wang, L. Ye, H. Luo, A. Men, F. Zhao, Y. Huang, "Pedestrian Stride-Length Estimation Based on LSTM and Denoising Autoencoders," *Sensors*, 19, 840, 2019.

[23] V. Bianchi, P. Ciampolini and I. De Munari, "RSSI-Based Indoor Localization and Identification for ZigBee Wireless Sensor Networks in Smart Homes," *IEEE Transactions on Instrumentation and Measurement*, vol. 68, no. 2, pp. 566-575, Feb. 2019, doi: 10.1109/TIM.2018.2851675.

[24] F. Zafari, A. Gkelias and K. K. Leung, "A Survey of Indoor Localization Systems and Technologies," *IEEE Communications Surveys*, vol. 21, no. 3, pp. 2568-2599, Apr. 2019,

[25] G. Huang, Z. Hu, J. Wu, H. Xiao, and F. Zhang, "WiFi and Vision Integrated Fingerprint for Smartphone-Based Self-Localization in Public Indoor Scenes," *IEEE Internet of Things Journal*, , Feb. 2020.

[26] M. Maheepala, A. Z. Kouzani, and M. A. Joordens, "Light-based Indoor Positioning Systems: A Review," *IEEE Sensors Journal*, Jan. 2020.

[27] J. J. P. Solano, S. Ezpeleta, and J. M. Claver, "Indoor localization using time difference of arrival with UWB signals and unsynchronized devices," *Elsevier: Ad Hoc Networks*, vol. 99, pp. 1–11, Mar. 2020.

[28] R. C. Luo, and T. Hsiao, "Indoor Localization System Based on Hybrid Wi-Fi/BLE and Hierarchical Topological Fingerprinting Approach," *IEEE Transactions on Vehicular Technology*, vol. 68, no. 11, pp. 10791–10806, Nov. 2019.

[29] S. Monfared, T. Nguyen, L. Petrillo, P. De Doncker, and F. Horlin, "Experimental Demonstration of BLE Transmitter Positioning Based on AOA Estimation," IEEE International Symposium on Personal, Indoor and Mobile Radio Communications (PIMRC), Bologna, Dec. 2018, pp. 856-859.

[30] P. Spachos, I. Papapanagiotou and K. N. Plataniotis, "Microlocation for Smart Buildings in the Era of the Internet of Things: A Survey of Technologies, Techniques, and Approaches," IEEE Signal Processing Magazine, vol. 35, no. 5, pp. 140–152, Sep. 2018.

[31] O. S. Eyobu, A. Poulose and D. S. Han, "An Accuracy Generalization Benchmark for Wireless Indoor Localization based on IMU Sensor Data," *2018 IEEE 8th International Conference on Consumer Electronics - Berlin (ICCE-Berlin)*, Berlin, 2018, pp. 1-3, doi: 10.1109/ICCE-Berlin.2018.8576213.

[32] J. Windau and L. Itti, *"Walking compass with head-mounted IMU sensor," 2016 IEEE International Conference on Robotics and Automation (ICRA), Stockholm, 2016, pp. 5542-5547.*

[33] X. Liu, N. Li, G. Xu and Y. Zhang, "A Novel Robust Step Detection Algorithm for Foot-mounted IMU," *IEEE Sensors Journal*, doi: 10.1109/JSEN.2020.3030771.

[34] S. Milici, A. Lazaro, R. Villarino, D. Girbau and M. Magnarosa, "Wireless Wearable Magnetometer-Based Sensor for Sleep Quality Monitoring," *IEEE Sensors Journal*, vol. 18, no. 5, pp. 2145-2152, March, 2018.

[35] J. Fang, H. Sun, J. Cao, X. Zhang, Y. Tao, "A novel calibration method of magnetic compass based on ellipsoid fitting," *IEEETrans*. Instrument. Meas., 60, 2053–2061, 2011.

[36] R. Harle, "A Survey of Indoor Inertial Positioning Systems for Pedestrians," *IEEE Communications Surveys & Tutorials,* vol. 15, no. 3, pp. 1281-1293, 2013.

[37] W. Kang and Y. Han, "SmartPDR: Smartphone-Based Pedestrian Dead Reckoning for Indoor Localization," *IEEE Sensors Journal*, vol. 15, no. 5, pp. 2906-2916, May 2015, doi: 10.1109/JSEN.2014.2382568.

[38] J. Luo and H. Gao, "Deep Delief networks for Fingerprinting Indoor Localization using Ultrawideband Technology," Int. J. Distrib. Sens. Netw., no. 18, 2016.

[39] C.S. Chen, "Artificial Neural Network for Location Estimation in Wireless Communication Systems," *Sensors*, vol. 12, pp. 2798-2817, 2012.

[40] D. Ramachandram and G. W. Taylor, "Deep Multimodal Learning: A Survey on Recent Advances and Trends," *IEEE Signal Processing Magazine*, vol. 34, no. 6, pp. 96-108, Nov. 2017.

[41] Z. Iqbal, D. Luo, P. Henry, S. Kazemifar, T. Rozario, Y. Yan, K. Westover, W. Lu, D. Nguyen, T. Long, J. Wang, H. Choy, and S. Jiang, "Accurate Real Time Localization Tracking in a Clinical Environment using Bluetooth Low Energy and Deep Learning," *arXiv/1711.08149*, 2017.

[42] M. Kulin, T. Kazaz, I. Moerman, and E. De Poorter, "End-to-End Learning From Spectrum Data: A Deep Learning Approach for Wireless Signal Identification in Spectrum Monitoring Applications," IEEE Access, vol. 6, pp. 18484-18501, Mar. 2018.

[43] M. Atashi, M. S. Beni, P. Malekzadeh, Z. HajiAkhondi-Meybodi, K. N. Plataniotis, and A. Mohammadi, "Orientation-Matched Multiple Modeling for RSSI-based Indoor Localization via BLE Sensors," Accepted in *28th European Signal Processing Conference (EUSIPCO)*, 2020.

[44] M. Atashi and A. Mohammadi, "Adaptive Online Dynamic Window(ODW) Assisted 2-stage LSTM Indoor Localization for Smart Phones," submitted to *2021 IEEE International Conference on Acoustics, Speech and Signal Processing*, 2021.

[45] A. Mohammadi and A. Asif, "Distributed Consensus+Innovation Particle Filtering for Bearing/ Range Tracking With Communication Constraints," *IEEE Trans. Signal Processing*, vol. 63, no. 3, pp. 620-635, 2015.

[46] A. Mohammadi and A. Asif, "Distributed Particle Filter Implementation With Intermittent/Irregular Consensus Convergence," *IEEE Trans. Signal Processing*, vol. 61, no. 10, pp. 2572-2587, 2013.

[47] M. Ozcan, A. Fuad, and G. Haluk, "Accurate and Precise Distance Estimation for Noisy IR Sensor Readings Contaminated by Outliers," Elsevier: Measurement, vol. 156, pp. 1–13, Feb. 2020.

[48] R. Carotenuto, M. Merenda, D. Iero, and F. G. D. Corte, "Mobile Synchronization Recovery for Ultrasonic Indoor Positioning," Sensors, vol. 20, no. 3, pp. 702–727, Jan. 2020.

[49] M. Maheepala, A. Z. Kouzani, and M. A. Joordens, "Light-based Indoor Positioning Systems: A Review," IEEE Sensors Journal, Jan. 2020.

[50] M.C. Cara, J.L. Melgarejo, G.B. Rocca, L.O. Barbosa and I.G. Varea, "An analysis of multiple criteria and setups for Bluetooth smartphone-based indoor localization mechanism," Journal of Sensors, 2017.

[51] YB. Bai, S. Wu, G. Retscher, A. Kealy, L. Holdend, M. Tomkoe, A. Borriakd, B. Hua, H.R Wuf and K. Zhang "A new method for improving Wi-Fi-based indoor positioning accuracy," Journal of Location Based Services 8, no. 3 (2014): 135-147.

[52] M. Khan, Y.D Kai,and H.U Gul "Indoor Wi-Fi positioning algorithm based on combination of Location Fingerprint and Unscented KaIman Filter " In Applied Sciences and Technology (IBCAST), 2017 14th International Bhurban Conference on (pp. 693-698). IEEE.

[53] Z. Wu, E. Jedari, R. Muscedere, R. Rashidzadeh, "Improved Particle Filter based on WLAN RSSI Fngerprinting and Smart Sensors for Indoor Localization," Computer Communications 83 (2016): 64-71.

[54] Z. Nan, Z. Hongbo, F. Wenquan, W. Zulin, "A novel particle Flter approach for indoor positioning by fusing WIFI and inertial sensors," Chinese Journal of Aeronautics, 28(6), pp.1725-1734.

[55] G. W. Samu, and P. Kadam, "Survey on Indoor Localization: Evaluation Performance of Bluetooth Low energy and Fingerprinting based Indoor Localization System," International Journal of Computer Engineering and Technology (IJCET), vol. 8, no. 6, pp. 23–35, Dec. 2017.

[56] J. J. P. Solano, S. Ezpeleta, and J. M. Claver, "Indoor localization using time difference of arrival with UWB signals and unsynchronized devices," Elsevier: Ad Hoc Networks, vol. 99, pp. 1–11, Mar. 2020.

[57] S. Weiguang, J. Du, X. Cao, Y. Yu, Y. Cao, S. Yan, and C. Ni, "IKULDAS: An Improved kNN-Based UHF RFID Indoor Localization Algorithm for Directional Radiation Scenario," Sensors, vol. 19, no. 4, pp. 968–986, Jan. 2019.

[58] Y. Gu and F. Ren, "Energy-Efficient Indoor Localization of Smart Hand-Held Devices Using Bluetooth," *IEEE Access* vol. 3, no. , pp. 1450-1461, 2015.

[59] P. Malekzadeh, A. Mohammadi, M. Barbulescu, and K. N. Plataniotis, "STUPEFY: Set-Valued Box Particle Filtering for Bluetooth Low Energy-Based Indoor Localization," *IEEE Signal Processing Letters*, vol. 26, no. 12, pp. 1773–1777, Dec. 2019.

[60] Y. Shu et al., "Gradient-Based Fingerprinting for Indoor Localization and Tracking," *IEEE Transactions on Industrial Electronics,*, vol. 63, no. 4, pp. 2424-2433, April 2016.

[61] S. Monfared, T. Nguyen, L. Petrillo, P. De Doncker, and F. Horlin, "Experimental Demonstration of BLE Transmitter Positioning Based on AOA Estimation," *IEEE International Symposium on Personal, Indoor and Mobile Radio Communications (PIMRC)*, Bologna, Dec. 2018, pp. 856-859.

[62] B. Yang, L. Guo, R. Guo, M. Zhao, and T. Zhao, "A Novel Trilateration Algorithm for RSSI-based Indoor Localization," Accepted in *IEEE Sensors Journal*, Mar. 2020.

[63] H. Zou, Z. Chen, H. Jiang, L. Xie and C. Spanos, "Accurate indoor localization and tracking using mobile phone inertial sensors, WiFi and iBeacon," *2017 IEEE International Symposium on Inertial Sensors and Systems (INERTIAL)*, Kauai, HI, 2017, pp. 1-4.

[64] A. Norrdine, Z. Kasmi and J. Blankenbach, "Step Detection for ZUPT-Aided Inertial Pedestrian Navigation System Using Foot-Mounted Permanent Magnet," *IEEE Sensors Journal*, vol. 16, no. 17, pp. 6766-6773, Sept.1, 2016, doi: 10.1109/JSEN.2016.2585599.

[65] J. Ruppelt, N. Kronenwett and G. F. Trommer, "A novel finite state machine based step detection technique for pedestrian navigation systems," *2015 International Conference on Indoor Positioning and Indoor Navigation (IPIN)*, Banff, AB, 2015, pp. 1-7, doi: 10.1109/IPIN.2015.7346771.

[66] A. Wang, X. Ou and B. Wang, "Improved Step Detection and Step Length Estimation Based on Pedestrian Dead Reckoning," *2019 IEEE 6th International Symposium on Electromagnetic Compatibility (ISEMC)*, Nanjing, China, 2019, pp. 1-4, doi: 10.1109/ISEMC48616.2019.8986071.

[67] M. S. Beni, Z. HajiAkhondi-Meybodi, M. Atashi, P. Malekzadeh, K. N. Plataniotis, and A. Mohammadi, "IoT-TD: IoT Dataset for Multiple Model BLE-based Indoor Localization/Tracking," *Accepted in 28th European Signal Processing Conference (EUSIPCO)*, 2020.

[68] A. Poulose and D. S. Han, "Indoor Localization using PDR with Wi-Fi Weighted Path Loss Algorithm," *2019 International Conference on Information and Communication Technology Convergence (ICTC)*, Jeju Island, Korea (South), 2019, pp. 689-693.

[69] P. Tadayon, T. Felderhoff, A. Knopp and G. Staude, "Fusion of Inertial and Magnetic Sensors for 3D Position and Orientation Estimation," *2016 38th Annual International Conference of the IEEE Engineering in Medicine and Biology Society (EMBC)*,Orlando, FL, 2016, pp. 3362-3365, doi: 10.1109/EMBC.2016.7591448.

[70] T. Feigl, S. Kram, P. Woller, R. H. Siddiqui, M. Philippsen and C. Mutschler, "A Bidirectional LSTM for Estimating Dynamic Human Velocities from a Single IMU," *2019 International Conference on Indoor Positioning and Indoor Navigation (IPIN)*, Pisa, Italy, 2019, pp. 1-8, doi: 10.1109/IPIN.2019.8911814.

[71] B. Wagstaff and J. Kelly, "LSTM-Based Zero-Velocity Detection for Robust Inertial Navigation," *2018 International Conference on Indoor Positioning and Indoor Navigation (IPIN)*, Nantes, 2018, pp. 1-8, doi: 10.1109/IPIN.2018.8533770.

[72] C. Yang, A. Mohammadi, and Q.W. Chen, "Multi-Sensor Fusion with Interaction Multiple Model and Chi-Square Test Tolerant Filter," *Sensors*, 16(11), 2016.

[73] H. W. Fentaw and T. Kim, *"Indoor localization using magnetic field anomalies and inertial measurement units based on Monte Carlo localization," 2017 Ninth International Conference on Ubiquitous and Future Networks (ICUFN), Milan, 2017, pp. 33-37.*

[74] P. Malekzadeh, A. Mohammadi, M. Barbulescu, and K.N. Pla-taniotis, "STUPEFY: Set-Valued Box Particle Filtering forBLE-based Indoor Localization *IEEE Signal Processing Let-ters*, 2019.